Aus dem Institut für Chirurgische Forschung
im Walter-Brendel-Zentrum für experimentelle Medizin
der Ludwig-Maximilians-Universität München
Vorstand: Prof. Dr. med. Ulrich Pohl

Characterization of a transgenic mouse expressing the reporter gene luciferase under the control of the murine early growth response-1 promoter

Dissertation
zum Erwerb des Doktorgrades der Medizin
an der Medizinischen Fakultät der
Ludwig-Maximilians-Universität zu München

vorgelegt von Philipp Sebastian Wilhelm Lukas Dußmann
aus München

2016

Mit Genehmigung der Medizinischen Fakultät

der Universität München

Berichterstatterin:	Priv. Doz. Dr. Elisabeth Deindl
Mitberichterstatter/innen:	Prof. Dr. Annette Nicke
	Priv. Doz. Dr. Roghieh Djafarzadeh Andabili
Dekan:	Prof. Dr. med. dent. Reinhard Hickel

Tag der mündlichen Prüfung: 25.02.2016

Contents

1. Introduction

1.1 Early growth response – 1

1.1.1 The Egr-1 gene and protein product

The transcription factor Early growth response – 1 (Egr-1) was discovered independently by several research laboratories and has been described by many different terms. Egr-1 was found first in human lymphocytes treated with concanavalin-A and cyclohexamide as a suspected regulatory cell cycle gene and was called G0S30 (Forsdyke 1985). Later, Milbrandt referred to the transcription factor as NGF inducible A (NGFI-A) due to its discovery after the stimulation of neuronal cells with nerve growth factor (NGF) (Milbrandt 1987). Other terms to describe Egr-1 include Zif268 (Zincfinger 268) (Christy and Nathans 1989), Krox24 (Krüppel Box 24) (Lemaire, Revelant et al. 1988), TIS8 (tetradecanoyl phorbol acetate-inducible *s*equence 8) (Lim, Varnum et al. 1987) CEF-5 (chicken embryo fibroblasts-5) (Simmons, Levy et al. 1989) and ZENK (zif-268; egr-1; NGFI-A; Krox-24) (Mello, Vicario et al. 1992). The current name Early growth response -1 (Egr-1) was first coined in 1988 by Sukhatme and Cao (Sukhatme, Cao et al. 1988). Soon after its discovery, the gene locus was mapped to human chromosome 5q23-31 (Sukhatme, Cao et al. 1988).

Within the 700 base pairs full length promoter region, located 5' upstream of the Egr-1-gene, five serum response elements (SRE) (Tsai-Morris, Cao et al. 1988) were identified, which account not only for the serum induced transcription, but also for the radioinducibility of Egr-1. All of those SRE sites contain the consensus sequence CC(A/T)GG, also known as 'CArG' element (Meyer, Kupper et al. 2002). Other regulatory elements identified within the promoter sequence are two cAMP responsive elements (CRE),

an activated protein-1/thiophorbolester responsive element (AP-1/TRE) (Meyer, Kupper et al. 2002) and two Egr-1 binding sequence (EBS) regions, which are thought to allow Egr-1 to regulate its own transcription (Cao, Mahendran et al. 1993). A schematic drawing of regulatory elements within the Egr-1 promoter sequence is shown in figure 1.

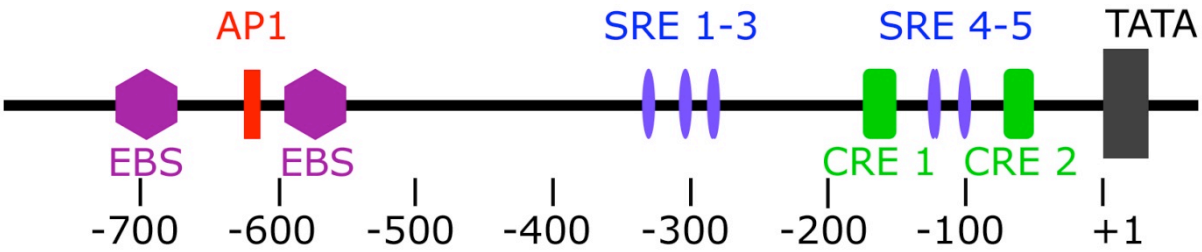

Figure 1: Schematic drawing representing the Egr-1 promoter sequence with regulatory elements: The human full-length Egr-1 promoter (700 bp) contains upstream of the TATA box two serum response elements (SRE 4, 5), flanked by one cAMP responsive element on each side(CRE 1, 2). Three more serum response elements (SRE 1-3), two Egr-1 binding sequences and activated protein-1 responsive element (AP 1) are mapped further upstream (adapted from (Meyer, Kupper et al. 2002))

Egr-1 mRNA kinetics were observed in various cell types after exposure to diverse activation stimuli. The transcripts are induced between 30 min and 1 h after cell activation and decline to basal concentration at 2 h (Keeton, Bortoff et al. 2003). Egr-1 protein kinetics were observed to follow the mRNA induction pattern with a 1 – 2 h delay. It was found that Egr-1 protein levels in vivo increase within 20 min, continue to be elevated at 1 to 2 h and descend back to basic levels by 4 h to 8 h (Cao, Koski et al. 1990; O'Donovan, Wilkens et al. 1998).

The Egr-1 gene encodes a 533-amino acid nuclear phosphoprotein (Lim, Varnum et al. 1987; Milbrandt 1987; Sukhatme, Cao et al. 1988), which belongs to the Egr family (Egr-1 to 4) of zinc finger proteins (Kharbanda, Nakamura et al. 1991; Patwardhan, Gashler et al. 1991). The three dimensional crystal structure of the Egr-1 protein was first shown by

Pavletich and Pabo (Pavletich and Pabo 1991). Later, it was revealed that the nuclear phosphoprotein product of Egr-1 contains three zinc fingers of the Cys_2His_2 class, which bind to their target DNA sequence 5'-CGCCCCCGC-3' in a zinc dependent manner (Cao, Koski et al. 1990; Gashler, Swaminathan et al. 1993). Each zinc finger domain consists of an alpha helix and an anti-parallel beta-pleated sheet. A representation of the protein structure of the Egr-1 zinc finger-DNA complex is shown in figure 2.

Figure 2: The protein structure of Zif 268 (Egr-1) Zinc Finger – DNA Complex, PDB-ID 1AAY, visualized from X-ray diffraction (Elrod-Erickson, Rould et al. 1996)

A bipartite nuclear localization signal (NLS) of Egr-1 was identified to reside within the basic residues 315 to 330 of the N-terminal sequence in addition to the second or third zinc finger (Gashler, Swaminathan et al.

1993), thus making the NLS dependent on the structure of the DNA binding domain (Matheny, Day et al. 1994).

The transcriptional co-repressors Nab 1 (NGFI-A binding protein 1) and Nab 2 have been found to have regulatory functions on Egr-1 by inhibiting its activity via direct protein - protein interaction. It was shown that this interaction is located within the central domain of the Egr-1 protein, which is presumably located within the residues 270 – 296 (Russo, Sevetson et al. 1995; Swirnoff, Apel et al. 1998). The modular structure of Egr-1 is represented in figure 3.

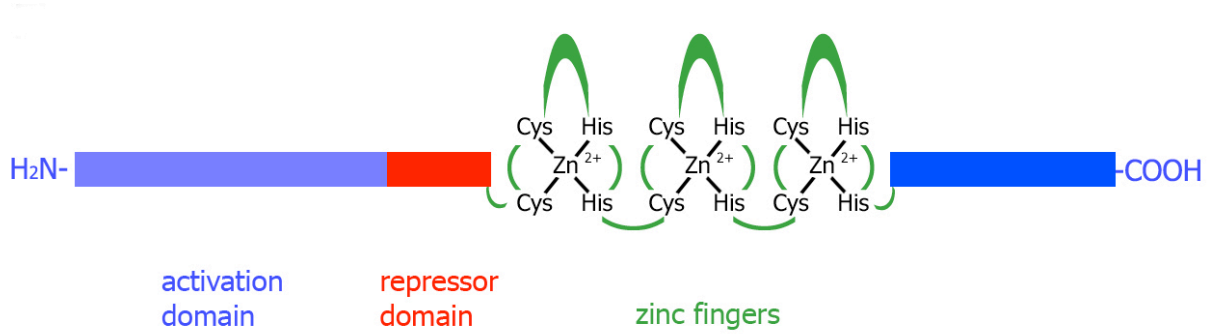

Figure 3: Modular structure of the zinc finger transcription factor Egr-1. The Egr-1 protein contains a transcriptional activation domain on the N-terminus followed by an inhibitory domain functioning as binding site for the transcriptional co-repressors Nab-1 and Nab-2. The DNA-binding domain consists of three zinc finger motifs. (adapted from (Thiel and Cibelli 2002)).

While Nab-1 is expressed constitutively, Nab-2 expression is induced by some of the same stimuli that also increase Egr-1 expression, such as serum or NGF stimulation (Svaren, Sevetson et al. 1996) and thereby prevents excessive activation of the Egr-1 target promoter. Additionally, Nab 2 is thought to be involved in a negative feedback loop, since Egr-1 itself is able to induce the expression of Nab 2 (Kumbrink, Gerlinger et al. 2005; Kumbrink, Kirsch et al. 2010).

Besides NGF, FGF1 (fibroblast growth factor 1), PDGF (platelet derived growth factor), VEGF (vascular endothelial growth factor), CBP (cAMP response element binding protein), p300 (Silverman, Du et al. 1998) and many other stimuli such as growth and differentiation factors, hormones, neurotransmitters, cytotoxic metabolites, cytokines, hypoxia (Yan, Lu et al. 1999), reactive oxygen intermediates and ionizing radiation (Datta, Taneja et al. 1993), UV radiation, death signals, tissue injury (Gashler and Sukhatme 1995; Thiel and Cibelli 2002) and other general serum proteins are also capable of activating Egr-1 (for a recent review see (J.I.Pagel 2010))

1.1.2 Egr-1 role and functions

Egr-1 is an important activator of a great number of target genes, which in turn are key players in differentiation, apoptosis and mitogenesis (Thiel and Cibelli 2002; Lee, Cho et al. 2004; Abdel-Malak, Mofarrahi et al. 2009). Being in the crossfire of different growth signals makes Egr-1 an interesting candidate to be studied during embryogenesis and neonatal development. Indeed Egr-1 activity has been detected in bones, whisker pads and teeth of developing mice embryos (McMahon, Champion et al. 1990).

To study the functions of Egr-1 in detail, Egr-1 knockout mice have been developed (Lee, Tourtellotte et al. 1995; Lee, Wang et al. 1996). Although Egr-1 knockout mice are viable, the females are sterile due to luteinizing hormone deficiency (Lee, Sadovsky et al. 1996; Topilko, Schneider-Maunoury et al. 1998; Tremblay and Drouin 1999).

Egr-1 has been shown to play an important role in an array of diverse physiological processes, such as the cholesterol biosynthesis in liver (Gokey, Lopez-Anido et al. 2011), the regulation of synaptic plasticity and long term memory formation (Jones, Errington et al. 2001; James,

Conway et al. 2006; Maddox, Monsey et al. 2011), reproduction (Topilko, Schneider-Maunoury et al. 1998), wound healing (Wu, Melichian et al. 2009), bone repair (Reumann, Strachna et al. 2011; Reumann, Strachna et al. 2011), persistent inflammatory pain (Ko, Vadakkan et al. 2005), or tissue survival following hypoxia (Yan, Lu et al. 1999; Nishi, Nishi et al. 2002).

A large amount of evidence for a crucial role of Egr-1 in the regulation of the immune response has also been found (McMahon and Monroe 1996) and binding sites within the promoter regions of genes coding for immune response proteins have been identified for TNFα (tumor necrosis factor α)(Kramer, Meichle et al. 1994), ICAM-1 (intercellular adhesion molecule 1) (Maltzman, Carmen et al. 1996), metallo-proteinases (Haas, Stitelman et al. 1999) and others. Moreover, the secretion of inflammatory mediators, such as Il-8, Il-13 or MMP-2 (matrix metalloproteinase – 2) from activated immune cells has been shown to rely on Egr-1 dependent mechanisms (Cho, Kang et al. 2006; Li, Ning et al. 2007; Ning, Dong et al. 2007).

Besides physiological processes, Egr-1 has been associated with a multitude of pathogenic processes, such as atherosclerosis (McCaffrey, Fu et al. 2000; Blaschke, Bruemmer et al. 2004), COPD (chronic obstructive pulmonary disease) (Shen, Gong et al. 2011), ALI (acute lung injury) (Copland, Kavanagh et al. 2003), diabetes (Hasan, Alshuaib et al. 2003; Hasan, Phukan et al. 2003), Alzheimer disease (Lu, Li et al. 2011), myopia (Schippert, Burkhardt et al. 2007), numerous viral infections (human immunodeficiency virus 1 (HIV-1) (Fan, Zou et al. 2011), mouse hepatitis virus (MHV) (Cai, Liu et al. 2006), herpes simplex virus-1 (HSV-1) (Bedadala, Palem et al. 2011)) or ethanol-induced fatty liver injury (McMullen, Pritchard et al. 2005). In addition, Egr-1 seems to be involved in tumor growth (Yang and Abdulkadir 2003) and was suggested to play various roles in neoplastic processes, such as colon carcinoma (Mahalingam, Natoni et al. 2010), gastric carcinoma (Zheng, Pu et al.

2010), lung carcinoma (Shimoyamada, Yazawa et al. 2010) or prostate carcinoma (Yang and Abdulkadir 2003).

In summary, recent research clearly showed that Egr-1 seems to play a central role in a multitude of diverse physiological and pathological processes alike and thus is an important gene to be studied.

1.2 The firefly luciferase

1.2.1 The luciferase (luc) gene and protein product

The firefly luciferase gene originates from the North-American firefly Photinus pyralis (Fig 4A) and consists of six introns, each less than sixty bases in length (de Wet, Wood et al. 1987). Its protein produces bioluminescence by catalyzing a light producing chemical reaction. The luciferase protein has a molecular weight of 62 kDa and contains an active site comprised of two separated domains: the larger first part is located at the N-terminal domain (residues 4 - 436) and the smaller second part at the C-terminal domain (residues 440 - 544)(Conti, Franks et al. 1996). The three dimensional protein structure was revealed by Conti and Franks (Conti, Franks et al. 1996) and is shown in figure 4B.

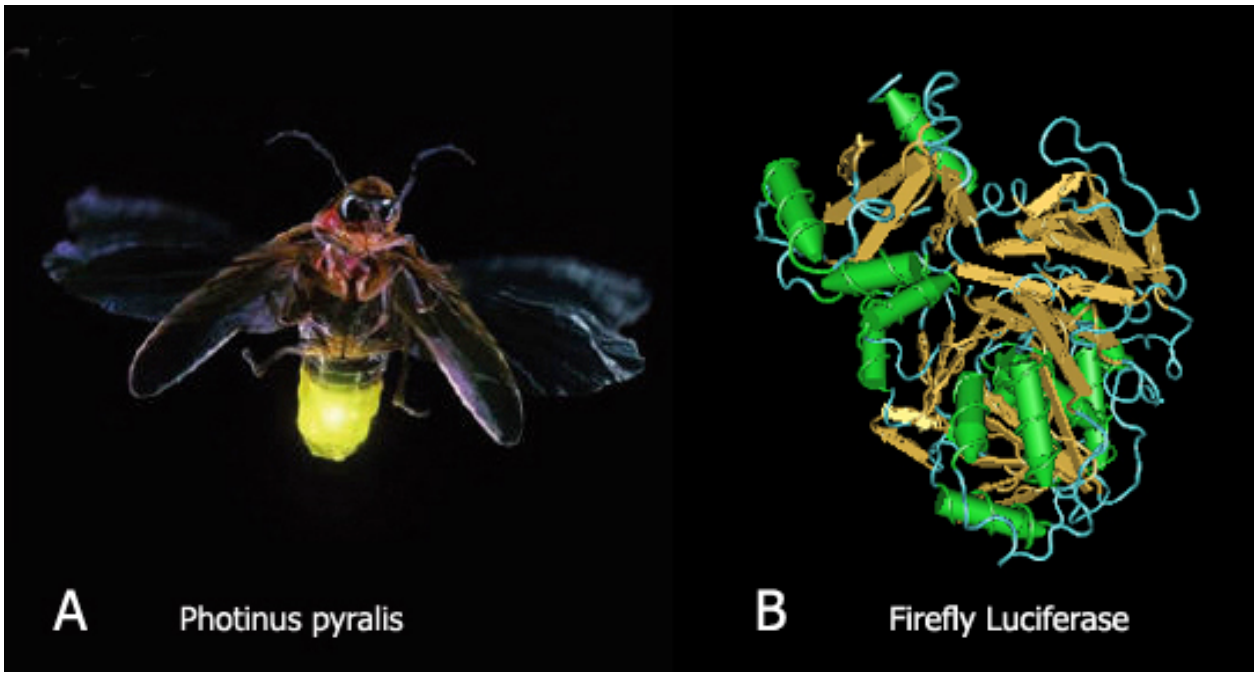

Figure 4: The firefly Photinus pyralis and the firefly luciferase

A The bioluminescent organism Photinus pyralis (adapted from (Rowe, Dikici et al. 2009))
B The protein structure of luciferase, visualized from X-ray crystallography (Conti, Franks et al. 1996)

The luciferase protein is found predominantly within the peroxisomes of cells due to a peroxisomal targeting signal, which is located at its extreme C-terminus (Gould, Keller et al. 1987).

The luciferase catalyzes the reaction of its unique substrate, named firefly luciferin. Luciferin is a benzthiazole and naturally only occurs in Photinus and Luciola fireflies (Greer and Szalay 2002). Biochemically, the firefly luciferase protein functions like a monooxygenase and catalyzes a two-step reaction: The reversible first step requires in addition to luciferin, ATP and magnesium and forms an enzyme bound luciferyl-adenylate. In the second step, the luciferyl-adenylate undergoes an oxidative decarboxylation using molecular oxygen. This results in the formation of carbon dioxide, oxyluciferin, AMP and light. The overall reaction is shown in figure 5.

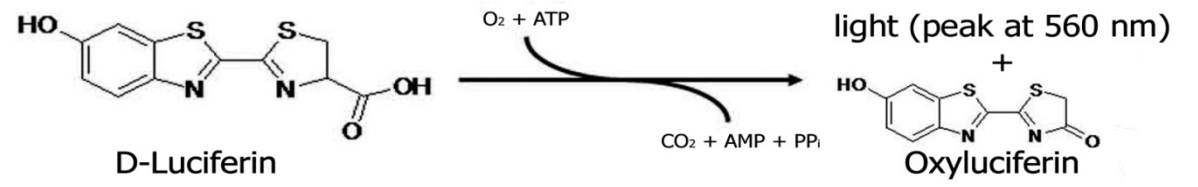

Figure 5: Light emitting reaction of the Photinus pyralis luciferase protein. The reaction depends on the cofactor Mg^{2+}, O_2 and ATP (adapted from (Waidmann, Bleichrodt et al. 2011))

The wavelength of emitted light is pH sensitive: At a pH 7.5 to 8.5, yellow-green with peak emission at 560 nm is emitted (de Wet, Wood et al. 1987), while the spectrum is shifted towards red at a more acidic pH *in vitro* (Viviani, Oehlmeyer et al. 2005). The pH dependent spectral changes are represented in figure 6.

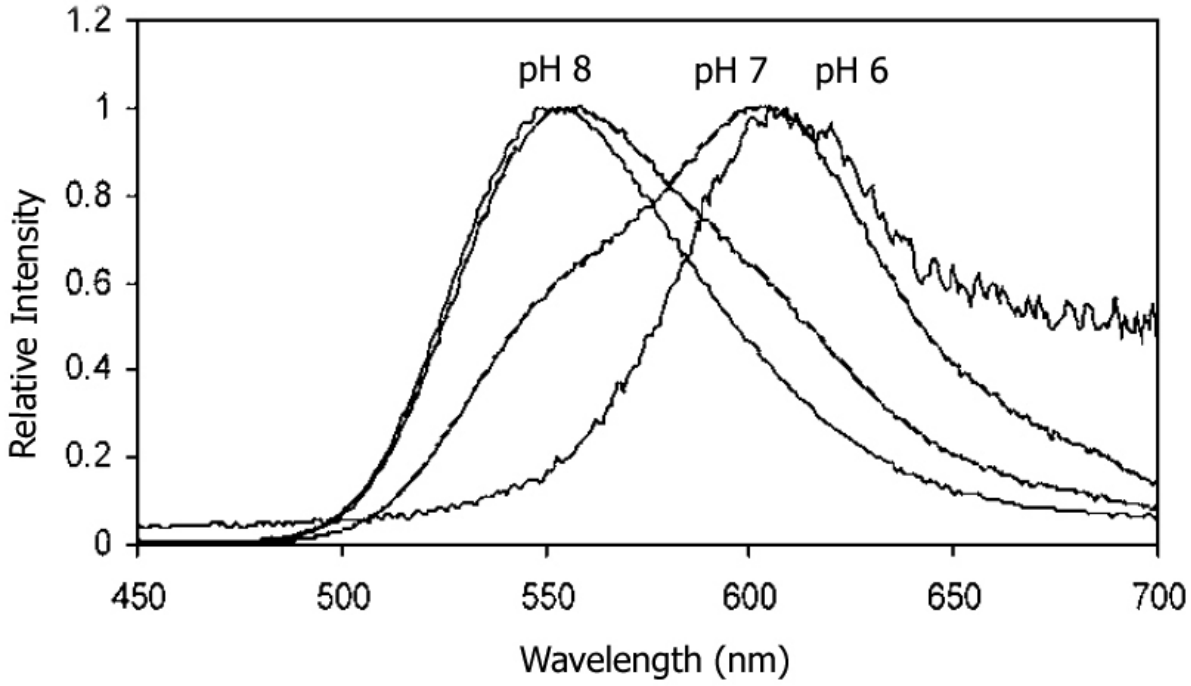

Figure 6: Bioluminescence spectra of Photinus pyralis luciferase at pH 6, pH 7 and pH 8 (adapted from (Viviani, Oehlmeyer et al. 2005)).

Mammalian cells can express the luciferase protein product after its gene has been incorporated into the cells genome. After exogenous addition of its substrate D-luciferin, which is rapidly distributed throughout the entire organism, bioluminescence of luciferases expressing cells with light in the wavelength range of 400-620 nm, at an emissions peak at 560 nm, can be observed (Rice, Cable et al. 2001; Ray, Pimenta et al. 2002).

1.2.2 Applications of luciferase

The nocturnal organism of Photinus pyralis uses its bioluminescence apparatus to emit specific light signals to communicate the species and sex of the signaler for mating purposes (Stanger-Hall, Lloyd et al. 2007). A multitude of scientific uses of firefly luciferases have emerged in recent

years. Through the use of luciferases, e.g. a widely spread standard assay to detect the presence of ATP or magnesium (Dumollard, Marangos et al. 2004) has been developed.

Firefly luciferases have also been proven to be a useful non-invasive tool for monitoring infections and drug treatment in living animals by the use of bioluminescent bacteria and viruses. Examples include the evaluation of antibiotic therapy on E. coli bacteria in a cutaneous wound model (Jawhara and Mordon 2004) and the study of intestinal colonization by E. coli (Foucault, Thomas et al. 2010), drug efficiency testing and *in vivo* monitoring of invasive Aspergillosis (Brock, Jouvion et al. 2008) or monitoring of herpes simplex virus type 1 (HSV-1) infection and therapy (Luker, Bardill et al. 2002).

Other applications include the monitoring of protein-protein interactions through the use of a split luciferase enzyme in living mice (Paulmurugan, Umezawa et al. 2002; Zhang 2004), together with luciferase complementation imaging (LCI) and bioluminescent optical imaging (Ray, Pimenta et al. 2002; Luker and Piwnica-Worms 2004).

Molecular imaging using luciferases has become a useful tool to continuously observe *in vivo* gene expression in human embryonic stem cells over a period of several weeks (Wilson, Yu et al. 2008) or the *in vivo* tracking of cells in cancer through vector-mediated gene expression (Shah, Jacobs et al. 2004).

Additionally, the firefly luciferase has been successfully utilized as a bioluminescent reporter in living mice using a photon imaging system for the noninvasive *in vivo* study of gene induction (Contag, Spilman et al. 1997) or the *in vivo* monitoring of circadian rhythms (Wilsbacher, Yamazaki et al. 2002).

In recent decades, luciferase imaging has been proven to be a useful tool for non-invasive monitoring of biologic processes not only in cell and tissue cultures, but also in living, multi-cellular organisms.

1.3 The Egr-luc mouse model

Previously, a transgenic mouse model using the murine full length Egr-1 promoter sequence to control the expression of the luciferase reporter was created in our lab. The construct containing the sequence from -930 to +237 base pairs relative to the Egr-1 promoter transcriptional start site of the murine Egr-1 promoter coupled to the reporter gene luciferase, was microinjected into the male pronucleus of mouse zygotes and was transferred into pseudo-pregnant females of C57Bl6 background. A schematic drawing of the construct used for generating Egr-luc transgenic mice is shown in figure 7. Presence of the transgene was confirmed by PCR analysis (Primer combination of the sequence between the luciferases gene and the SV40 small-t intron) (Vogel 2003).

Figure 7: Schematic drawing of the construct used for generating transgenic mice: The murine full-length Egr-1 promoter (1200 bp) was linked to the reporter gene luciferase followed by the SV40 small-t intron (adapted from (Vogel 2003)).

Seven founder animals were obtained from this construct and breeding with wild-type animals of C57Bl6 strain yielded the establishments of two lines (L1 and L2) that were further propagated. All Egr-1-luc transgenic mice were healthy and viable with a normal life span with no display of any malformations in consequence of the presence of the transgene (Vogel 2003).

1.4 Rationality of the studies

Most data on Egr-1 gene activation have been evaluated only within *in vitro* studies and could not be confirmed when reevaluated *in vivo* (J.I.Pagel 2010). For this reason, it is inevitably necessary to study activation patterns and their time course in the living organism. In knockout mice, however, the relatively mild phenotype suggests that compensation of Egr-1 loss of function by other Egr family members cannot be excluded. Moreover, Egr-1 activation is subject of rapid alteration due to its sensitivity to many external stimuli. Transcriptional modifications are easily prone to external and environmental manipulations, including growth and differentiation factors, hormones, neurotransmitters, cytotoxic metabolites, cytokines, hypoxia, UV radiation, death signals or tissue injury (Gashler and Sukhatme 1995; Thiel and Cibelli 2002). This suggests that Egr-1 could possibly also be induced without intention by the investigator and dynamic changes over time cannot be examined satisfactory by end-point measurements. Therefore, a long-term observatory and noninvasive approach could greatly enhance the possibilities of gaining new qualitative and quantitative information on *in vivo* Egr-1 gene activation.

1.5 Aim of the thesis

The aim of this thesis was the characterization of the transgenic Egr-1-luc murine model. First, it had to be established that this model is working as designed and that both proteins, the Egr-1 and luciferase protein products, are expressed and transcribed simultaneously without competitively inhibiting each other. To exemplary validate the suitability of primary cells cultured from Egr-1-luc mice for *in vitro* monitoring of Egr-1 activity, I isolated and cultured smooth muscle cells from aortic tissue to measure

Egr-1 promoter activity quantitatively using luciferase luminescence. It then had to be validated if this model is suitable for the qualitative and quantitative study of Egr-1 expression patterns over time in the living animals. To verify this, I applied this model to study Egr-1 promoter driven luciferase expression during the development of neonatal mice between the ages of 7 - 21 days after birth to observe Egr-1 promoter activity over time. I followed the temporal and spatial activation pattern of Egr-1 during wound healing and tissue regeneration in a model for wound healing of ear tissue and in a model for liver regeneration after one-third liver hepatectomy. To confirm the body luminescence imaging (BLI) data obtained, I visualized luciferases and Egr-1 activity using immunohistochemical analyses in regions of interest in mice embryos as well as in the liver tissue of the same animals used prior for BLI prior. I carried out additional analyses of the protein and mRNA levels in liver tissue, using Western blot and quantitative Real-time Polymerase Chain Reaction respectively, to further validate the BLI data of liver regeneration.

2. Materials and Methods

2.1 In vivo experiments

2.1.1 Materials and equipment

- -20°C Refrigerator (Bohmann, Kempen)
- Aqua ad iniectabilia Diaco® (Braun, Melsungen)
- Carprofen (Pfitzer, Berlin)
- Disposable Scalpel (Feather, Japan)
- D-Luciferin (Promega, Hilden)
- Ear notcher (Napox) (Heiland, Hamburg)
- Ethanol (Merck, Darmstadt)
- Ethylene diamine tetra-acetic acid (EDTA) (Biochrom, Berlin)
- Fentanyl (Janssen-Cilag, Neuss)
- Formaldehyde (Merck, Darmstadt)
- Histosette® embedding cassettes (Simport, Canada)
- Isoflurane (Abbott, Wiesbaden-Delkenheim)
- IVIS™ Lumina Imaging System (Caliper Life Sciences GmbH, Mainz)
- Midazolam (Ratiopharm, Ulm)
- Medetomidine Dorbene® Vet (Pfitzer, Berlin)
- Phosphate buffered saline (PBS) (Sigma-Aldrich, Steinheim)
- Sodium-chloride solution (B. Braun, Melsungen)
- Surgical instruments (Dumont Medical; FST, USA)
- Sutures:
    - Ethicon Prolene 4.0 (Johnson & Johnson, USA)
    - Ethicon Sutupak Silk 4.0 (Johnson & Johnson, USA)
    - Ethicon Vicryl Sutures 5.0 (Johnson & Johnson, USA)
- Syringes (Braun, Melsungen)

- Vaporizer: VIP 3000® Isoflurane (Midmark, USA)
- XGR-8 Gas Anesthesia System (Caliper Life Sciences GMBH, Mainz)
- Xylazin Rampun® 2 % (Bayer, Leverkusen)

2.1.2 Animals

The Egr-1-luc transgenic mice of C57BL/6 background were housed in individually vented cages with a 12h day/night cycle with chow and water provided *ad libitum*. Male and female mice at different ages were used for the experiments. All animals were given adequate care and all animal procedures were approved and controlled by the local ethics committee and carried out according to the institutional guidelines and in compliance with the guidelines of the German law for protection of animal life.

2.1.3 The Egr-luc murine model

Transgenic Egr-luc mice were generated previously in our laboratory (Vogel 2003). For this purpose, 1200 bp of the murine full-length Egr-1 promoter sequence was cloned into the plasmid pUHC13-2 replacing the CMV promoter in the CMV-Luc expression cassette. The vector containing the murine Egr-1 promoter was a generous gift from Martin Braddock (Glaxo Wellcome, United Kingdom). From this vector, the Egr-1 promoter (Tsai-Morris, Cao et al. 1988) compassing the sequence from -930 to +237 base pairs relative to the Egr-1 promoter transcriptional start site (Gius, Cao et al. 1990; Schwachtgen, Houston et al. 1998) was isolated by SalI restriction. 5' ends were filled-in with DNA polymerase I (Klenow enzyme) and cloned into the pUHC13-2 vector by blunt end ligation thereby replacing the CMV promoter. The pUHC13-2 vector, which was a generous gift from H. Bujard (ZMBH, Germany), is a derivate of

pUHD10-1 (Deuschle, Pepperkok et al. 1989) and was originally developed by U. Baron in the laboratory of H. Bujard. In short, the reporter plasmid pUHC13-2 containing the promoter-enhancer sequence of the CMV promoter followed by a polylinker and the luciferase gene of *Photinus pyralis* (firefly) fused to the SV40 small-t intron and poly(A) signal was digested with HindIII and XhoI to excise the CMV promoter. The 5'ends were filled in with Klenow enzyme and ends were dephosphorylated with alkaline phosphatase. After cloning the Egr-1 promoter into pUHC13-2 vector, the Egr-1 promoter - luciferase reporter gene - SV40 small-t intron fragment was isolated by AseI and PvuI digestion. Finally the transgene was purified using a QIAquick Gel Extraction Kit (Qiagen). All constructs obtained were reviewed and verified by sequencing. Transgenic mice were established by microinjecting the plasmid into male pronuclei (identified by size) of murine zygotes and transferred into pseudo-pregnant females (strain C57BL6). The presence of the transgene was confirmed by means of PCR using a specific primer combination spanning the region between the reporter gene luciferase and the SV40 small-t intron (forward primer: 5'- GAG ATC GTG GAT TAC GTC GC - 3'; reverse primer: 5'- TGC TCC CAT TCA TCA GTT CC -3'). For the Egr-1-luciferase construct seven founder animals were obtained. Breeding of founder animals with wild-type mice (C57Bl6, Harlan) led to an establishment of two lines (L1 and L2) that were bred further using exclusively animals that tested positive for luciferase expression by luminescence. Egr-1-luc transgenic mice are viable and healthy and show a normal life span, indicating no serious malformation due to the presence of the transgene. Breeding capabilities were also normal with a litter size of 5 - 8 pups, indicating no serious loss of function of the Egr 1 gene product.

2.1.4 In vivo imaging of luciferase activity

In vivo imaging for bioluminescence was performed using the IVIS™ Lumina Imaging System (Caliper Life Sciences GmbH, Mainz). The images were acquired by a CCD-Camera, thermoelectrically cooled to -90°Celsius for optimal results, in a light-tight imaging chamber and on a movable heat-controlled stage. The bioluminescence signal was collected for one to three minutes, depending on the bioluminescence intensity. Reflected light pictures were taken during illumination with four white LEDs. Image acquisition and processing was carried out using Living Image 2.60.1 – IGOR Pro 4.09 Software. An illustration of the IVIS™ imaging system is provided in figure 8.

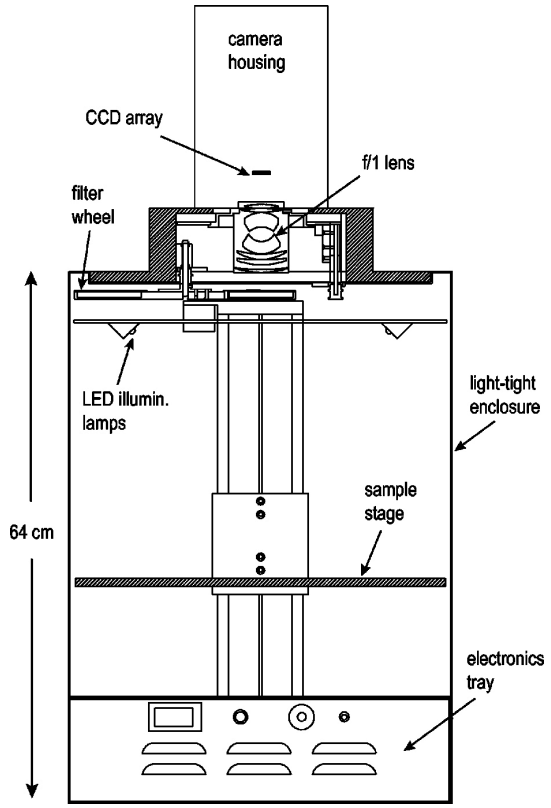

Figure 8: Illustration of the IVIS™ imaging system (Rice, Cable et al. 2001)

For the developmental studies, Egr-1-luc transgenic mice were anesthetized by i.p. injection of xylazin/ketamin/luciferin (0.375, 0.635 and 100 µl D-luciferin in PBS, respectively). For the one-third liver hepatectomy model, the animals were anaesthetized by administration of isoflurane by a gas manifold with a flow rate of 2.0 % during treatment at indicated time points and received 50 µl carprofen and 100 µl D-luciferin (60mg/ml D-Luciferin diluted in PBS) by i.p. injection. After 8 – 9 min, the animals were killed by cervical dislocation and the body cavity was opened immediately thereafter. BLI from the exposed liver were collected 10 min after luciferin injection. As a control, the exposed livers of sham operated animals were measured.

For the ear wound healing model, the animals were anaesthetized by administration of isoflurane and received 100 µl D-luciferin (60mg/ml D-Luciferin diluted in PBS) by i.p. injection. BLI from the ear region was carried out 10 min after luciferin injection. The ear was immobilized with adhesive tape during imaging. As a control, the untreated ear was measured.

2.1.5 One third liver hepatectomy

Hepatectomy was carried out based on a protocol by Mitchell and Willenbring (Mitchell and Willenbring 2008) with slight modifications. Mice were anaesthetized by administration of isoflurane and were injected i.p. with 50 µl carprofen for pain reduction. All surgical steps were carried out as described (Mitchell and Willenbring 2008), except that only the median liver lobe was resected. For this, the ventral skin was sterilized by the application of 70 % ethanol solution. The liver was exposed by a 2.5 – 3.0 cm long midline abdominal incision through the skin and muscle tissue and made accessible by the use of a rubber band under the xiphoid process and special retractors. The organ was pushed down using a saline moistened cotton tip and the falciform ligament was cut with

microsurgery scissors. The ligament connecting the caudate and left lateral lobe was cut in a similar fashion. A 4.0 thread was placed on the base of the median lobe above the gall bladder, but at least 2 mm from the suprahepatic vena cava, and knotted. The lobe was resected with microsurgery scissors directly above the knotted part, only leaving a small ischemic stump behind. The peritoneum and skin were sutured using 4.0 threads. The mice were allowed to awake at 100 % oxygen flow and were carefully evaluated for 20 to 30 minutes. After surgery, mice received i.p. injections of 50 µl carprofen daily for pain reduction. In control animals, only the midline abdominal incision was performed and sutured. At indicated time points after surgery, animals were anaesthetized, the liver was exposed by laparotomy and images of the ventral view of the fully exposed liver were collected.

2.1.6 Collection of mice embryos

The mother animal was euthanized by an overdose of narcotics (Midazolam, Medetomidine, Fentanyl) at the indicated developmental stage of the embryos and the uterus was surgically exposed by midline abdominal incision and opened. The mice embryos were collected in embedding cassettes (Histosette) and stored over night in formaldehyde solution. The embryos were then transferred into EDTA solution and stored for 2 weeks until further processing.

2.1.7 Ear wound healing model

A punch wound of approximately 1.5 mm in diameter was inflicted with an ear notcher on one ear of Egr-1-luc animals according to the standard procedure of animal labeling. 24 h after the wound setting, BLI from the ear region was carried out. As a control, the untreated ear was measured.

2.2 In vitro experiments

2.2.1 Materials and equipment

- -80°C Refrigerator: Herafreeze® (Thermo Scientific, USA)
- -20°C Refrigerator (Liebherr, Biberach an der Riss)
- 4°C Refrigerator (Liebherr, Biberach an der Riss)
- 12 well culture cluster (Corning incorporated, USA)
- 24 well culture cluster (Corning incorporated, USA)
- Acetic acid (Merck, Darmstadt)
- AequoriaMDSTM Macroscopic Imaging System (Hamamatsu, Herrsching am Ammersee)
- Amphotericin B (Sigma-Aldrich, Steinheim)
- ATP (Roche, Mannheim)
- BCA Proteinassay Kit (Pierce; Thermo Scientific, IL, USA)
- Camera: Hamamatsu 1394 ORCA-ERA (Hamamatsu, Herrsching am Ammersee)
- cDNA Synthesis Kit for RT-PCR (Roche, Mannheim)
- Cell Culture dishes (TPP, Switzerland)
- Cell lysis solution (Promega, Mannheim)
- Centrifuge 5424 (Eppendorf, Weseling)
- Centrifuge Micro 200R (Hettich, Tuttlingen)
- Chloroform/isoamylalcohol (49:1) (Fluka, Deisenhofen)
- CoA (Sigma-Aldrich, Steinheim)
- Collagenase II (Sigma-Aldrich, Steinheim)
- Disposable scalpel (Feather, Japan)
- D-luciferin (Promega, Mannheim)
- Dry milk (Merck, Darmstadt)
- DTT 1,4-dithiothreitol (Sigma-Aldrich, Steinheim)
- Ethylene diamine tetra-acetic acid (EDTA) (Biochrom, Berlin)
- Ethylene glycol-bis tetra-acetic acid (EGTA) (Sigma, Munich)

- Ethanol (70%, 96%, 100%) (Merck, Darmstadt)
- Fetal Calf Serum (10 %) (Gibco, Darmstadt)
- Gelatin (Merck, Darmstadt)
- Gel blot paper (Whatman, Great Britain)
- GelCode blue staining reagent (Pierce; Thermo Scientific, USA)
- Glutamine (Biochrom, Berlin)
- Glycerol (Merck, Darmstadt)
- Gradient-gel (Serva, Heidelberg)
- Guanidine (Sigma, Munich)
- Guanidine Thiocyanate (Sigma, Munich)
- HAM's F12 medium (Biochrom, Berlin)
- Hydrogen Peroxide (Merck, Darmstadt)
- Horseradish peroxidase (HRP) conjugated rabbit polyclonal antibody against firefly luciferase (1:1000) (Santa Cruz Biotechnology, USA)
- Incubator CB53 (Binder, Tuttlingen)
- Isopropanol (Sigma, Munich)
- Potassium chloride (Merck, Darmstadt)
- Laemmli-buffer 10x (Serva, Heidelberg)
- Lithium Chloride (Sigma, Munich)
- Light Cycler 1.5 (Roche, Mannheim)
- Light Cycler® FastStart DNA Master^{Plus} SYBR Green I Kit (Roche, Mannheim)
- M199 Medium (Biochrom, Berlin)
- MaXtract High Density containers (Quiagen, USA)
- Mercaptoethanole (Sigma, Munich)
- Methanol (Merck, Darmstadt)
- Magnesiumchloride (Merck, Darmstadt)
- Microscope (Zeiss, Oberkochen)
- Microtome model MED H_n40 (Leica Microsystems, Bensheim)
- Sodium fluoride (Sigma, Munich)
- Nitro-cellulose-membrane (Pierce; Thermo Scientific, USA)
- N-Lauroylsarcosine sod. Salt (Sigma, Munich)

- Non-fat dry milk (Bio-Rad Laboratories, Munich)
- Nonamers (Roche, Mannheim)
- Ponceau Sodium Salt (Santa Cruz Biotechnology, Inc., USA)
- Penicillin 10000 IE (Biochrom, Berlin)
- Phenol (Sigma, Munich)
- Phenylmethylsulfonyl fluoride (PMSF) (Boehringer, Ingelheim am Rhein)
- Phosphate buffered saline (PBS) (Sigma-Aldrich, Steinheim)
- Photometer: BioPhotometer (Eppendorf, Weseling)
- Pipettes 10,20,100,200,1000µl (Eppendorf, Weseling)
- Poncau-S-color solution (Sigma, Munich)
- Potassium-chloride (Merck, Darmstadt)
- Rabbit monoclonal antibody against Egr-1 (1:500) (Cell Signalling, USA)
- Rabbit monoclonal antibody against β-actin (1:2000) (Sigma, Munich)
- Recombinant luciferase (Promega, Mannheim)
- Restore western blot stripping buffer (Pierce; Thermo Scientific, USA)
- RQ1 RNase-free DNase (Promega, USA)
- Scale: RET Basic (IKA Labortechnik, Staufen)
- Sodium-acetate (anhydrous) (Sigma, Munich)
- Sodium bicarbonate (Gibco, Darmstadt)
- Sodium citrate tribasic dihydrate (Sigma, Munich)
- Sodium orthovanadate (Sigma, Munich)
- Sonicator: Ultrasonic Processor XL® (Heat Systems, USA)
- Streptomycin (Biochrom, Berlin)
- Sucrose (Sigma, Munich)
- Super Signal West Femto Maxim 1 kit (Pierce; Thermo Scientific, USA)
- Surgical micro scissors (Dumont Medical; FST, USA)

- Tris buffered saline buffer 10x: 24.2g Tris base (Applichem, Darmstadt), 80 g NaCl (Applichem, Darmstadt), 165 ml 1M HCl (Merck, Darmstadt), 835 ml distilled water
- Thiocyanate (Sigma, Munich)
- Tris-glycine gel (4–20%) (Serva, Heidelberg)
- Tris-Hydrochloric acid: 1M Tris buffer (Applichem, Darmstadt) and HCl (Merck, Darmstadt)
- Triton X-100 (Sigma-Aldrich, Steinheim)
- Trypsin (Biochrom, Berlin)
- Tube luminometer (Lumat LB 9507, Berhold Technologies, Bad Wildbad).
- Tween (0.1%) (New England Biolabs, USA)
- Waterbath (GFL, Burgwedel)
- Waymouth (Gibco, Darmstadt)
- Xylol (Merck, Darmstadt)

2.2.2 Cell culture

Primary cultures of murine aortic smooth muscle cells (SMC) were established as previously described (Pelisek, Armeanu et al. 2001). Male and female mice were killed by an overdose of narcotics (midazolam, medetomidine, fentanyl) and the ascending and descending aorta was removed. Fat and surrounding tissues were removed with a disposable scalpel under a microscope (Zeiss, Oberkochen) and the aorta was cut lengthwise with micro scissors. The tissue pieces were incubated with a small amount of enzyme solution (0.1 % collagenase II, 0.1 % trypsin diluted in PBS) for 20 min at 27°C. The solution was exchanged with a small amount of M199 medium and the endothelial cells were detached and removed by gently scraping the surface and pipetting the solution up and down several times. The aortic tissue was cut into small sections and the tissue pieces were placed on gelatin coated plates and covered with 1

ml of culturing solution after adhesion (standard HAM's F12/Waymouth 1:1 medium, 10 % FCS (fetal calf serum), 4 mM glutamine, 100 U penicillin, 100 µg/ml streptomycin, 2.5 mg/ml amphotericin B) for outgrowth of SMC's. The medium was exchange every 24 to 36 hours. After the SMC's were growing out, the tissue pieces were removed and the cells were split. The cells were seeded into gelatin coated twelve-well plates with the same medium for culturing. Cells were cultured at 37°C in a 5 % CO_2 humidified atmosphere. For stimulation, cells between passages three and four were serum starved for two days.

2.2.3 Luciferase assay

Smooth muscle cells were harvested at a confluence of 70 – 90 % by trypsination, collected by centrifugation for 10 min at 1000 rpm and lysed for 20 to 30 min in 0.5x lysis buffer solution at room temperature. Quantification of luciferase activity was performed in cell lysates as described (Ogris, Carlisle et al. 2001). For quantification, an aliquot of cell lysate was quantified using a tube luminometer (Lumat LB 9507, Berhold Technologies, Bad Wildbad). Measurements were taken with an integration time of 10 sec, following a lag time of 2 sec after the injection of the luciferases assay reagent (LAR; 20mM glycylglycine, 0.1 mM EDTA, 3mM DTT, 0.55 mM ATP, 0.3 mM CoA, 0.5 mM D-luciferin, pH 8.5). As control of the background auto-florescence level, the values of wild-type cells were measured and deducted from the measurement; two ng recombinant luciferase (Promega) correspond to 10^7 relative light units (RLU).

2.2.4 RNA isolation

Total RNA was isolated based on a protocol by Chromzynski and Sacchi (Chomczynski and Sacchi 1987) with slight modifications from frozen liver samples 12 h after hepatectomy or sham operation (n=4). For RNA extraction, 30 mg tissue specimen were mechanically homogenized with 600 µl denaturing solution, containing 4 M guanidinium thiocyanate, 25 mM sodium citrate, pH 7.0, 0.5 % (wt/vol) *N*laurosylsarcosine (sarkosyl) and 0.1 M 2-mercaptoethanol. The denaturing solution was prepared by dissolving 367,6 mg 25 mM sodium citrate tribasic dehydrate, pH 7, in 50 ml distilled water, adding 23,6 g 4 M guanidine thiocyanate, 0.25 g 0.5 % N-lauroylsarcosine sodium salt/50 ml and 50 ml 0.1 M 2-mercaptoethanol. A 2 M sodium acetate solution was prepared by adding 16.42 g anhydrous sodium acetate to 40 ml water and 35 ml glacial acetic acid pH 4 (glacial acetic acid brought to a final volume of 100 ml with water) for the next step. After transfer of the tissue into a polypropylene tube, 60 µl 2 M sodium acetate solution, pH 4, 600 µl water-saturated phenol and 120 µl chloroform/isoamylethanol (49:1) were added sequentially, shaking the mixture for 1 min after addition of each ingredient to ensure thorough mixing of the organic and acidic-aqueous phase. The entire volume was transferred into 2 ml MaXtract high-density containers, cooled for 15 min on ice and centrifuged for 2 min and 12000 rpm at 4°C. The upper aqueous phase was transferred into a 1.5 ml tube and 1 µl glycogen and 600 µl isopropanol were added to precipitate the RNA. After storage over night at -20°C, the pellet was collected by centrifugation for 30 min and 12000 rpm, re-suspended in 1 ml 70 % ethanol to wash the RNA and recovered by centrifugation for 5 min. and 12000 rmp. The pellet was re-suspended in 90 µl denaturing solution (as described above), 90 µl isopropanol were added to precipitate the RNA and the mixture was stored for 1 hour or over night at -20°C. The pellet containing the isolated RNA was collected by centrifugation for 20 min and 12000g and

was re-suspended in 48 µl water. The isolated total RNA was incubated at 37C° for 30 min after the addition of 6 µl 10x TBS buffer and 6 µl DNAse (RQ1 RNase-free DNase 1000 U, 1U/µl). The reaction was stopped by the addition of 140 µl water and incubation for 10 min at 65°C. 100 µl phenol and 100 µl chloroform/isoamylalcohol (49:1) were added, the volume was transferred into 2 ml MaXtract high density containers, cooled on ice for 15 min and centrifuged for 2 min and 1200g at 4°C). The supernatant was transferred into a 1.5 ml tube, 300 µl isopropanol and 30 µl 4 M Lithium-Chloride were added to precipitate the RNA and the mixture was stored for 1 hour at -20°C. The pellet was collected by centrifugation for 15 min and 13000 rpm at 4°C, washed twice using 1 ml 70 % ethanol (as described above) and allowed to dry for 10 min at room temperature. For further processing, the dry pellet was re-suspended in 100 µl water and incubated for 15 min at 64°C to ensure complete solubilization. To measure the concentration of the total RNA in the sample and to estimate purity, spectrophotometric readings at wavelength of 260 nm and 280 nm were obtained using a photometer (BioPhotometer, Eppendorf).

2.2.5 Quantitative real time Polymerase Chain Reaction (qRT-PCR)

One microgram of DNAse treated total RNA was reverse transcribed using random nonamers (Roche, Mannheim) and a 1st Strand cDNA Synthesis Kit for RT-PCR (Roche, Mannheim). qRT-PCR was performed with a Light Cycler 1.5 (Roche, Mannheim) in a reaction volume of 10µl using a Light Cycler® FastStart DNA Master^{Plus} SYBR Green I Kit (Roche, Mannheim) and 50 pmol of each primer (Egr-1, forward: 5´- CGA ACA ACC CTA TGA GCA CCT G – 3´; reverse: 5´- CAG AGG AAG ACG ATG AAG CAG C – 3´; luciferase, forward: 5´- CAG ATG CAC ATA TCG AGG TG – 3´; reverse: 5´- CAT ACT GTT GAG CAA TTC ACG – 3´; 18s rRNA, forward: 5´- GGA CAG GAT TGA CAG ATT GAT AG – 3´; reverse: 5´- CTC GTT CGT TAT CGG AAT TAA C – 3´). Three independent qRT-PCR reactions were

performed on each template. An initial denaturation step at 95°C for 10 min was followed by 40 cycles of denaturation (95°C, 10 sec), annealing (64°C for Egr-1; 58°C for luciferase, 64°C for 18S rRNA, 5 sec), and extension (72°C, 15 sec). Melt curve analyses were performed to control specific amplification. Results were normalized to the expression levels of the 18S rRNA.

2.2.6 Western blot

Total and nuclear protein extracts of liver tissue samples were isolated 48 h after hepatectomy as described (Barancik, Htun et al. 2000). The liver tissue samples were unfrozen and mechanically homogenized in 3 ml ice-cold buffer solution, containing 0.1 mM sodium orthovanadate, 1 mM Phenylmethylsulfonyl fluoride (PMSF), pH 7.4, 1 mM dithiothreitol (DTT), 1 mM EDTA, 1 mM EGTA, 10 mM potassium-chloride, 50 mM tris-hydrocloric acid and 250 mM sucrose. 1 ml of the homogenate was centrifuged for 10 min and 4000 rpm at 4°C and the supernatant was collected. The supernatant after this step contained the soluble cytosolic protein fraction. The pellet was re-suspended in a buffer containing 0.5 mM PMSF, pH 7.4, 1 mM EGTA, 1 mM DTT, 1 mM EDTA, 10 mM potassium-chloride, 10 mM NaF, 50 mM tris-HCl and 1000 mM sucrose and homogenized on ice using a sonicator (Ultrasonic Processor XL, Heat Systems). The mixture was centrifuged for 30 min and 13000 rpm at 4°C and the recovered pellet was re-suspended in a buffer containing 0.1 mM sodium orthovanadate, 0.1 % Triton X-100, 0.5 mM PMSF, 1.0 mM DTT, 1.0 mM EGTA, 10 % glycerol, 50 mM Tris-HCl and 400 mM KCl. The mixture was mechanically homogenized on ice to yield the nuclear protein fraction. 4x laemmli buffer (10x laemmli buffer containing 0.25 M Tris, 1.92 M Glycine and 1 % SDS in aqueous solution) was added, the proteins were heat-denatured for 5 min at 95°C, cooled on ice and centrifuged at 13000 rpm for 1 min to prepare the probe for western blot

analysis. Equal amounts of protein were separated on a 4–20 % Tris-glycine gel at a voltage of 10 mA/gel for 10 min, followed by 25 mA/gel for 70-90 minutes. 1x laemmli buffer was used as electrophoresis buffer. After electrophoresis, the buffer was removed and the gel cassette taken out. The gel was exposed, equilibrated together with Whatman gel blot paper and the nitrocellulose membrane for 5 min in transfer buffer (Tris-base, glycine, SDS, methanol, water) and assembled from anode to cathode. A voltage of 104 mA was applied for 1 hour to transfer the protein from the gel to the nitrocellulose membrane. After transfer, the membrane was dyed with Ponceau-S solution and washed using a washing buffer solution (PBS – Tween (0.1 %)), until bands became visible. After documentation, the washing process was continued until the bands disappeared and the membrane was blocked with 5 % dry milk in washing buffer (as described above). The membrane was washed with TBS washing buffer three times for 10 min respectively. Immunoreactive bands were visualized using Super-Signal-Femto-West (Pierce) with a HRP conjugated rabbit polyclonal antibody against firefly luciferase (1:1000, Santa Cruz Biotechnology), a rabbit monoclonal antibody against Egr-1 (1:500, Cell Signaling) or β-actin (1:2000, Sigma), respectively. Luminescence was evaluated using Hamamatsu 1394 ORCA-ERA camera, AequoriaMDSTM Macroscopic Imaging System and Wasabi software (Hamamatsu Photonics, Herrsching, Germany). Protein bands were quantified by densitometry, and results expressed as Luc/ß-actin and Egr-1/ß-actin ratio, respectively. For negative control, the first antibody was omitted. Blots were repeated at least twice.

2.3 Immunohistochemistry

2.3.1 Materials and equipment

- 4°C Refrigerator (Liebherr, Biberach an der Riss)
- Aminoethyl carbazole (AEC) single solution, (Invitrogen, USA)
- Anti-luciferase goat polyclonal horseradish peroxidase (HRP) conjugated antibody (1:50) (Abcam, United Kingdom)
- Camera: AxioCam HRm (Zeiss, Oberkochen)
- Citrate-buffer: 5,882 g Tri-Sodium-Citrate (Merck, Darmstadt) in 2000 ml distilled water, buffered with 6 mol HCl solution to pH 6
- Embedding cassettes Histosette (Simport, Canada)
- Embedding-machine: Shandon Citadel 1000 (Thermo Fisher Scientific, USA)
- Ethanol (70%, 96%, 100%) (Merck, Darmstadt)
- Haemalaun stain (Roth, Karlsruhe)
- Histosette (Simport, Canada)
- Hotplate (Severin, Sundern)
- Hydrogen peroxide (Merck, Darmstadt)
- Luciferase goat polyclonal horseradish peroxidase (HRP) conjugated antibody (1:50) (Abcam, United Kingdom)
- Methanol (Merck, Darmstadt)
- Microscope Axiovert 200 (Zeiss, Oberkochen)
- Microtome model MED H_n40 (Reichert-Jung, Bensheim)
- Paraffin wax Paraplast plus (Sigma-Aldrich, USA)
- Paraformaldehyde (PFA, 4%)(Merck, Darmstadt)
- Phosphate buffered saline (PBS) (Merck, Darmstadt)
- Pipettes 10,20,100,200,1000µl (Eppendorf, Weseling)
- Pronase E (Merck, Darmstadt)
- Sakura® Tissue TEC® TEC™ (Sakura, Leiden)
- Scale: RET Basic (IKA Labortechnik, Staufen)

- Shandon cover plates (Thermo Scientific, USA)
- SuperFrost^{TM} Slides (Thermo Fisher Scientific, USA)
- Tris-buffer: 60,58g Trisma base (Sigma, Munich) solved in 400ml distilled water, buffered with N HCl solution to pH 7.5 and diluted to 1000 ml with distilled water
- Tween 20 (Sigma-Aldrich, USA)
- Water bath (GFL, Burgwedel)
- Ultramount (Dako, Hamburg)
- Vectastain Elite ABC Kit (Rabbit IgG) (Vektor, CA, USA)
- Xylene (Roth, Karlsruhe)

2.3.2 Formalin fixation and paraffin embedding

For immunhistochemical detection of luciferase and Egr-1, the harvested liver tissue was fixed in 4 % paraformaldehyde (PFA) over night at 4°C and subsequently embedded in paraffin. Embryos (n = 6, littermates) were collected at day 14 of development for detection of luciferase and Egr-1. They were transferred into embedding cassettes (Histosette) immediately after removal and stored in 4 % PFA solution for 24 to 48 h for fixation. They were placed in a solution of Na_4EDTA (ethylenediaminetetraacetic acid tetrasodium salt), 200 g/L, pH 7.1 (adjusted using 20 % w/v citric acid) at room temperature for 14 days to ensure decalcification. The embryos and the liver tissue were rinsed for 1 hour with running water and stored in 70 % ethanol until further processing. The embedding-machine (Shandon Citadel 1000, Thermo Scientific) was prepared by filling the respective tanks with 70 % ethanol, 96 % ethanol, xylene and paraffin wax Paraplast Plus. The samples were automatically dehydrated and embedded in paraffin wax by bathing them in a graded alcohol series (twice (2 hours and 1 hour) in 70 % ethanol, once (1.5 hours) in 80 % ethanol, once (1.5 hours) in 90 % ethanol,

twice (1.5 and 1 hours) in 96 % ethanol, twice (1.5 and 1 hour) in pure alcohol) bathing them twice (1.5 and 1 hour) in xylene and twice in 60°C warm paraffin wax (Paraplast Plus). The tissues were then stored 60°C warm paraffin wax until embedment into a paraffin block using the Sakura® Tissue TEC® TEC™ system.

After cooling down to room temperature, the embedded tissues were cut into 4 µm thick sections, flattened in a 40°C warm water bath and mounted on the specimen slides (SuperFrost™ microscope slides). The specimen slides were allowed to dry overnight at 37°C before staining.

2.3.3 Egr-1 dyeing

The dried specimen slides were de-pariffinized twice for 15 min in xylene, rehydrated in a graded alcohol series (5 min each in pure ethanol, 96% ethanol and 70 % ethanol) and rinsed for a short time with distilled water. Egr-1 antigen retrieval was performed in a steamer with sodium citrate buffer (5,882 g tri-sodium-citrate in 2000 ml distilled water), pH 6.0 – adjusted using 6 mol HCl solution) for 20 min and rinsed for 5 min with PBS/Tween. Endogenous peroxidase activity was quenched by treatment with 3 % hydrogenperoxide (3 ml H_2O_2, 180 ml methanol) for 5 minutes before being transferred on Shandon cover plates. For Egr-1 staining, slides were incubated over night at 4°C with a rabbit anti-mouse antibody (1:50 in PBS/Tween). Slides were rinsed with PBS/Tween (3 min) and incubated with a secondary antibody from the rabbit ABC kit (VECTASTAIN® Elite ABC system, Vector) according to the manufacturer's instructions. Immunoreactivity was visualized with the chromogen 3-amino-9-ethyl-carbazole (AEC single solution) for 20 min. As negative control the primary antibody was omitted.

2.3.4 Luc dyeing

The dried specimen slides were de-pariffinized as described above. Antigen retrieval for luciferase staining was achieved with Pronase E diluted in 0.5 M Tris buffer (1mg Pronase E in 1 ml Tris-buffer) for 15 min at room temperature and rinsed for 5 min with PBS/Tween (0.1%). Peroxidise blockage was performed as described above before the samples were mounted on Shandon coverplates.

Slides were incubated over night at 4°C with a polyclonal goat-anti-luciferase horseradish peroxidase (HRP) conjugated antibody (Abcam, 1:50 in Tris-buffered saline (TBS). Immunoreactivity was visualized with the chromogen 3-amino-9-ethyl-carbazole solution (AEC single solution) for 20 minutes and rinsed in PBS/Tween. The tissue was counterstained with haemalaun (10 sec) to visualize the cell nuclei, rinsed in water and sealed with Ultramount.

Pictures were taken on a Zeiss Axiovert 200 microscope with a Zeiss AxioCam HRm camera, using 20x objective (Zeiss) and 4x/10x lenses (Zeiss).

2.4 Software

- Adobe Photoshop CS 3
- Living Image 2.60.1 – IGOR Pro 4.09 Software
- Microsoft Office Word 2007
- Microsoft Office Excel 2007
- Wasabi software (Hamamatsu Photonics, Herrsching, Germany)

2.5 Statistics

All statistical analyses were performed using WinStat. p-values <0.05 were regarded as statistical significant and calculated using either the non-parametric U-test (according to Mann-Whitney) or the Wilcoxon test.

3 Results

3.1 Cell culture

Vascular smooth muscle cells (SMC) isolated form aortic tissue of adult Egr-1-luc mice were cultured *in vitro* and the luciferase activity measured in cell lysates to analyze exemplary, whether or not primary cells from Egr-luc mice might also be suitable for *in-vitro* investigations. On average, 4,000 RLU were measured per well (12-well plate, background value of luc-negative cells >300 RLU/well).

3.2 The Egr-luc murine model

Transgenic Egr-1 - luc mice were generated previously in our laboratory (Vogel 2003). To show functional expression of luciferase, adult Egr-1-luc mice were injected with the luciferase substrate D-luciferin and the activity monitored by BLI in anaesthetized animals. A representative image is shown in figure 9.

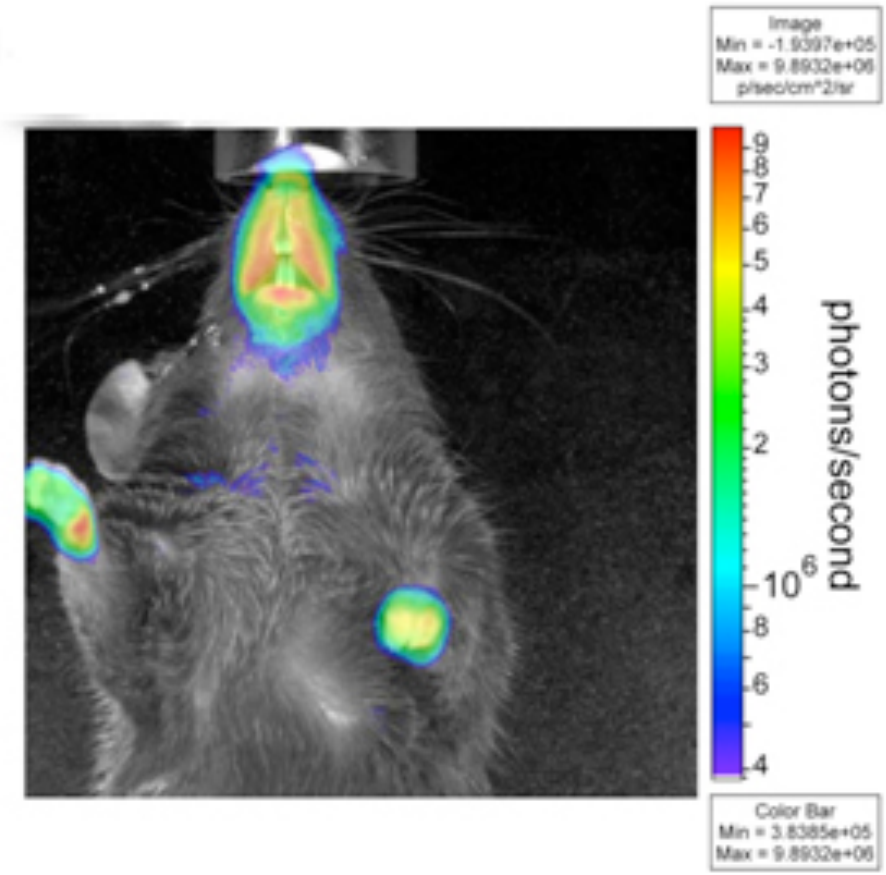

Figure 9: Luciferase activity in adult Egr1-luc mouse

Transgenic Egr1-luc mice (16 weeks old, male or female) were anaesthetized by administration of isoflurane and received 6 mg luciferin in 100 µl PBS by i.p. injection. 10 min after injection BLI measurement was carried out (1 min signal collection, setting 'high resolution'). A representative animal is shown. The reflected light picture is overlaid by a color-coded BLI image visualized in 'blend mode', which allows allocating the BLI signal to the respective areas shown in the underlying reflected light picture.

In the living animal, highest signal intensities were observed in regions around the snout (especially lips), ears and paws, whereas luciferase signal in other regions was not detectable. The absence of signal detection in fur-covered regions could partly be due to quenching effects.

3.3 In vivo monitoring of Egr-1 promoter activity during postnatal development and embryogenesis

To monitor expression of the reporter during postnatal development, Egr-1-luc transgenic mice were imaged at 7, 10, 13, 16, 19 and 21 days after birth. Day 7 was the earliest possible date for the i.p injection of the anesthetic and luciferase. Animals from the same litter were measured for luciferase activity on indicated dates and were kept with the parent between the measurements to ensure feeding by lactating mother animals. For luciferase signal quantification we used defined regions of interest (ROI), which were placed over the snout and paw of the mice. Due to the lack of hair growth, which otherwise could reduce the luciferase signal and interfere with signal quantification, we did not expect significant signal quenching. The total number of photons collected per area was normalized to background levels by subtraction of the total counts per area measured in an equal sized ROI placed over a background area of the same picture. As shown in figure 10A, mice showed strong luciferase expression throughout the entire ventral side of the body at day 7 after birth. A clear reduction of overall luciferase activity, including paws, snout, ears and tail, was observed during their development throughout the next 2 weeks. When quantifying the luciferase signal in ROI's at paw (Fig 10B) and snout (Fig 10C), luciferase activity was found to be reduced over time reaching 30 or 40 %, respectively, at day 21 compared to the initial value at day 7.

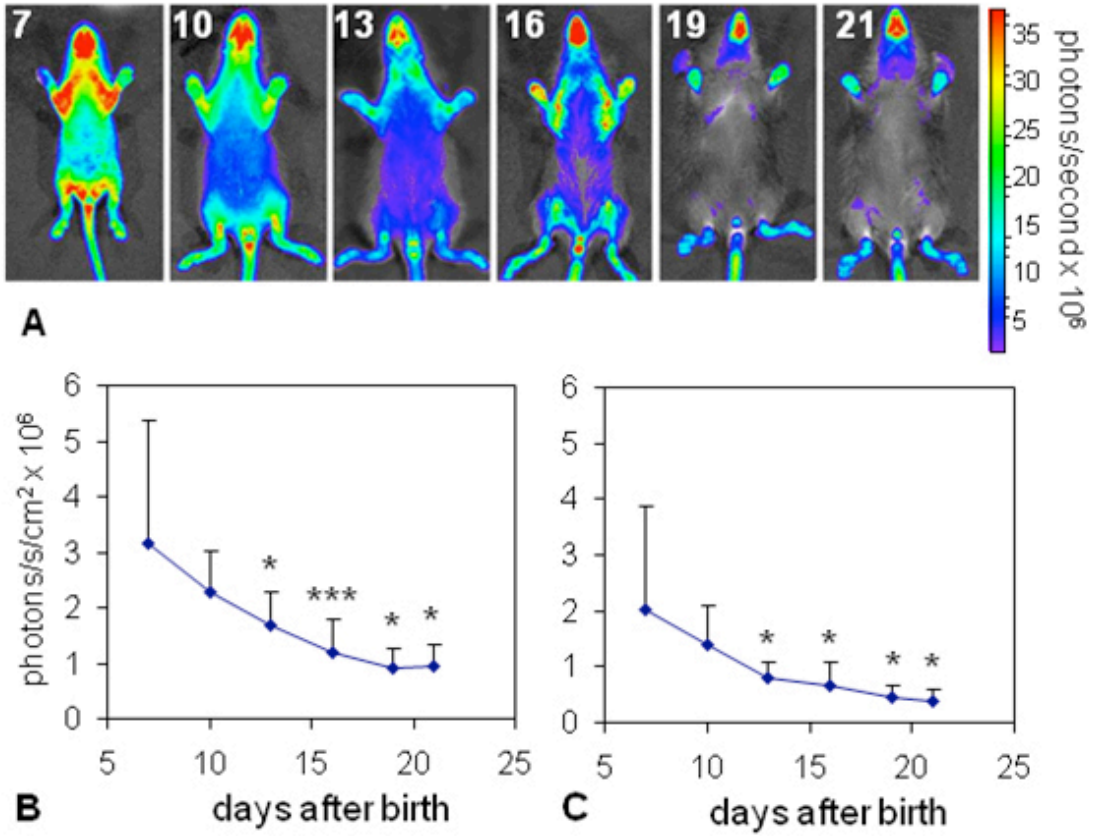

Figure 10: Egr-1 promoter driven luciferase activity during postnatal development (day 7 - 21 after birth)

Luciferase activity in Egr-1-Luc mice at indicated age (days after birth) was measured by bioluminescence imaging (BLI) after i.p. injection of D-luciferin. Luciferase signal was collected for 10 sec from the ventral side of the mice. (n=6)

A: A reflected light picture of representative animals at indicated age is overlaid by a color-coded BLI image. The numbers on the upper left indicate the age in days after birth. **B and C:** Luciferase activity was quantified within regions of interest (ROI's) placed at the paw (B) or snout area (C) and expressed as photons per second per cm^2 to correct for size differences in ROI size at different ages. A background ROI of equal size was subtracted. Median values of six animals + standard deviation are shown. * $p < 0.05$, *** $p < 0.001$; indicated day vs. day 7, Wilcoxon test.

3.4 Embryonic development: immunohistochemical analyses

I evaluated Egr-1 promoter activity in transgenic and non-transgenic embryos on day E14 of development (Theiler Stage 22) by immunohistochemical analyses of luciferase (Fig 11). In accordance with the BLI data obtained from the Egr-1-luc transgenic mice, bone primordia of hind limbs stained positive for luciferase (Fig 11A). Various neuronal structures demonstrated luciferase activity but it was mainly located at the sympathetic paravertebral ganglia (Fig 11B). Furthermore, an intense immunoreactivity was detected at the masticatory apparatus, especially at the area of the palatal shell (Fig 11C); snout and whisker follicles showed only slight staining (data not shown). The tissue specimens of non-transgenic control animals did not display any positive staining for luciferase (Fig 11D-F). When staining sections with anti Egr-1 antibody, a comparable pattern to luciferase staining could be observed, as for example at the masticatory apparatus (Fig 11G).

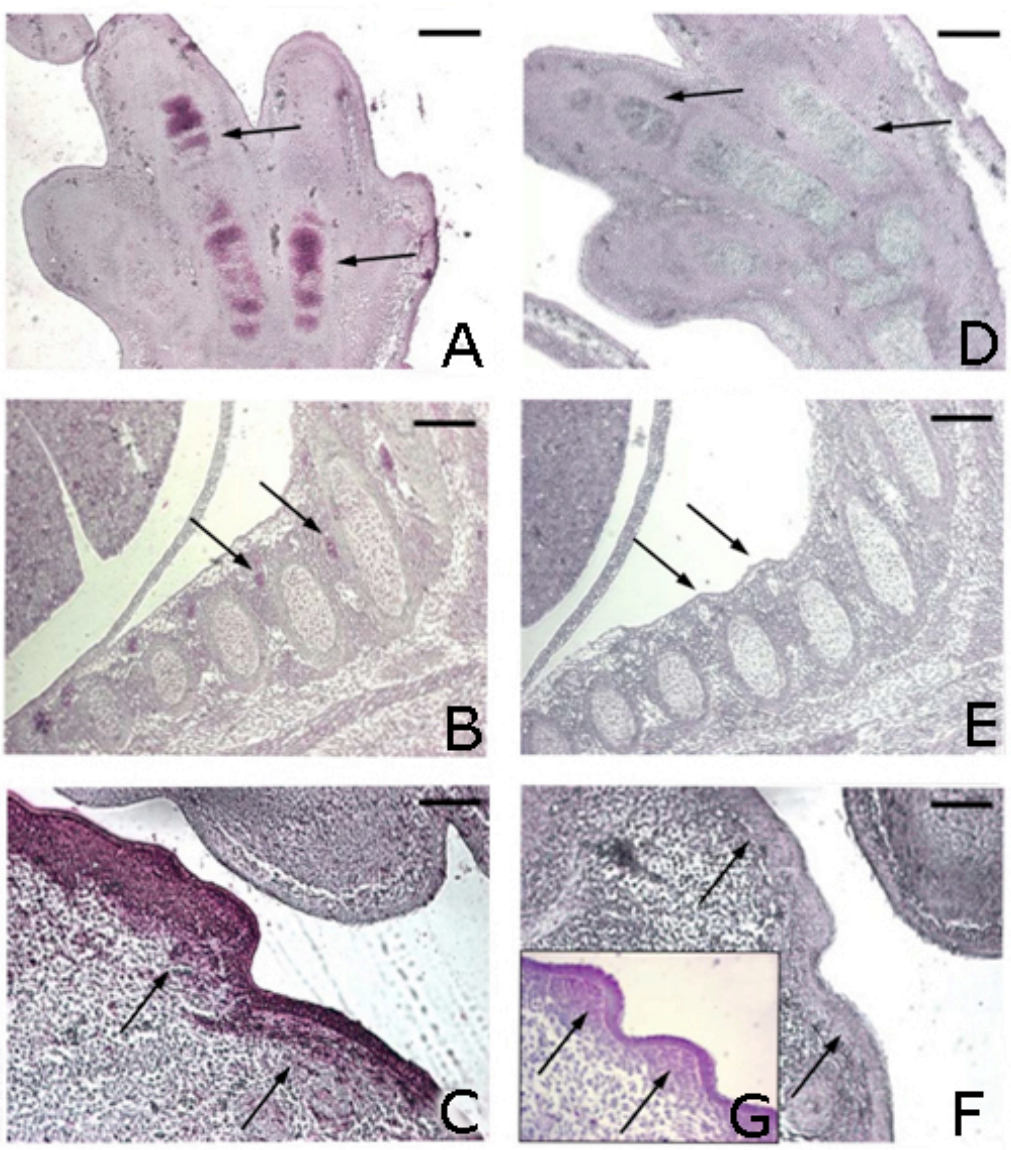

Figure 11: Immunohistochemical analyses of luciferase and Egr-1 expression during embryonic development

Egr-1-luc (A, B, C and G) and wild type (D, E and F) C57BL/6 embryos on day E14 of development were stained for luciferase protein (A-F) or Egr-1 protein (G). In bone primordia of hindlimbs (A, D), sympathetic paravertebral ganglia (B, E) and masticatory apparatus (C, F) luciferase positive areas (arrows) are stained in lilac in transgenic embryos (A-C), in wild-type embryos no luciferase signal is detected (D-F). When staining for Egr-1 protein, a similar pattern of protein expression is found in the masticatory apparatus (G) as for luciferase (C); scale bar: 50 µm

3.5 Hepatectomy

3.5.1 Egr-1 activation in regenerating liver

Liver hepatectomy in rodents leads to induction of cell division in the majority of hepatocytes 1-2 days after surgery (Fausto, Campbell et al. 2006). Here, I used *in vivo* BLI to verify at first that Egr-1 promoter activity can be monitored within the opened abdominal cavity of the Egr-1-luc transgenic mice and to show that no Egr-1 promoter activity was detectable in the untreated liver tissue of 1 month old mice, as shown in figure 12.

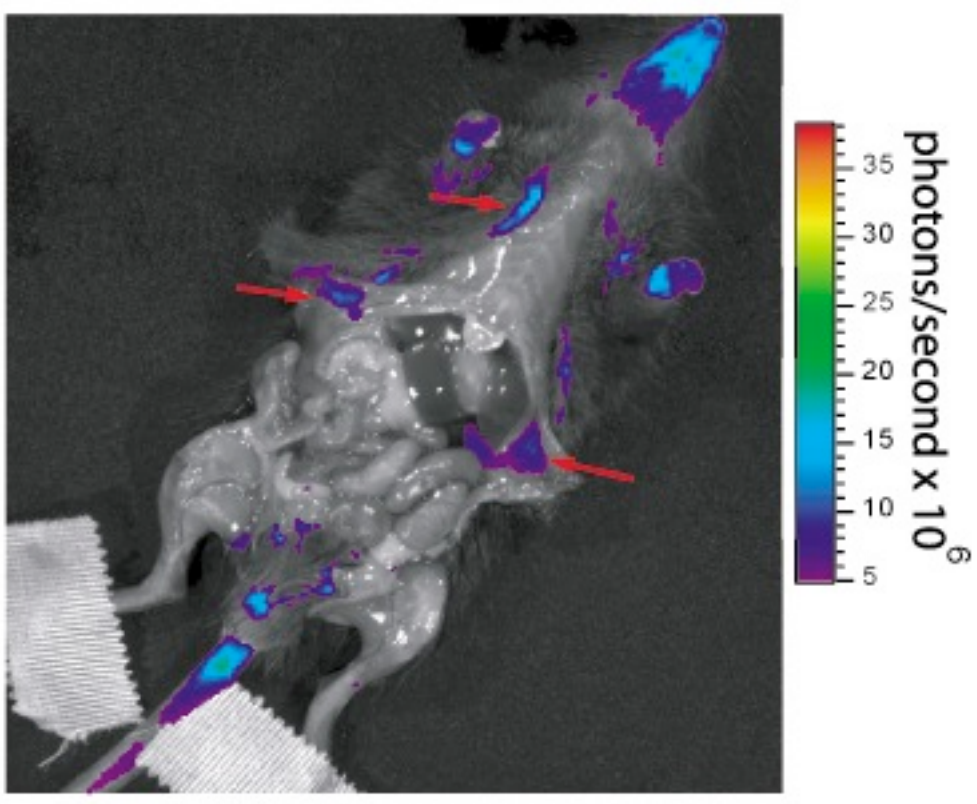

Fig. 12: BLI of adult Egr-1-luc mice with opened body cavity.

Transgenic Egr-1-luc mice (one month old) received 6 mg luciferin in 100 µl PBS by i.p. injection. After 10 min, the animal was killed by cervical dislocation, the body cavity opened immediately, skin from the ventral side partially removed and BLI measurement was carried out (10 min signal collection, setting 'high resolution'). A representative animal is shown.

I then used the same method to monitor the activity of the Egr-1 promoter in the transgenic mice 48 h (n=6 and n=3 control) and 72 h (n=4 and n=3 control) following one-third hepatectomy. For quantification purposes, ROI's were placed over the areas of regenerating liver tissue close to the primary excision site. The highest Egr-1 activity was observed at regions directly adjacent to the original sectioning wound with some elevated activity at the edges of the liver lobes, as shown in figure 13A.

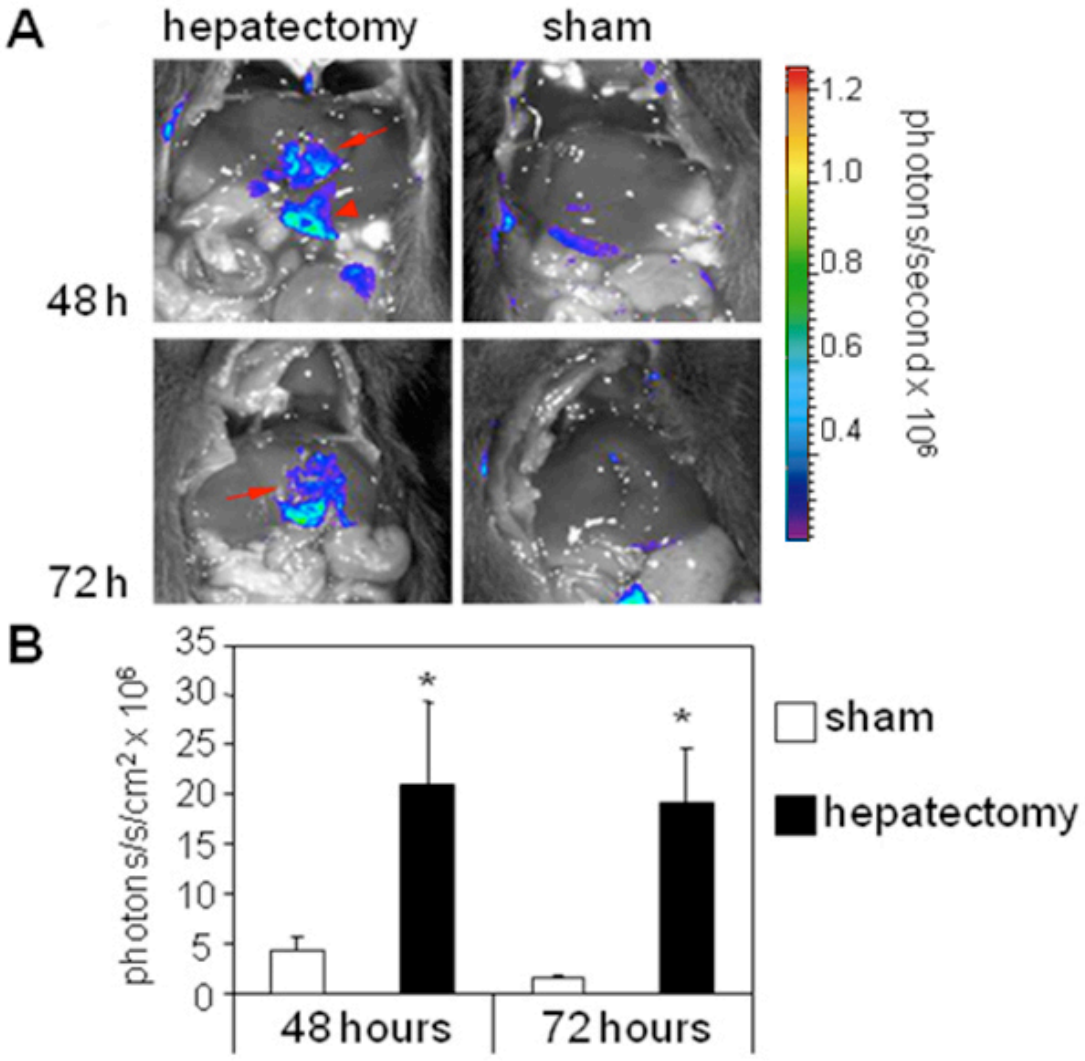

Figure 13: Egr-1 promoter driven luciferase activity after partial liver hepatectomy

A: BLI of hepatectomized (left) or sham operated (right) Egr-1-luc mice at 48 h (top row) and 72 h (bottom row) after surgery; representative animals from n = 3 - 6 are shown. Red arrows denote the site of initial surgery, arrowhead points at the edge of a liver lobe showing luciferase activity.

B: Quantitative luciferase signals from ROI's placed over the liver area of sham operated or hepatectomized animals 48 h and 72 h after surgery. A representative background ROI of equal size was subtracted to account for background activity. n = 3 - 6; * $p<0.05$ sham vs. hepatectomy (U-test, Mann-Whitney)

When quantifying the BLI signal in the area next to the excision site, an up to 12-fold signal increase was observed compared to sham operated animals, both at 48 h and 72 h after surgery (Fig 13B). Clusters of cells stained positive for Egr-1 (Fig 14A) and for luciferase (Fig 14B) were observed in section of liver tissue at the site of surgery after hepatectomy.

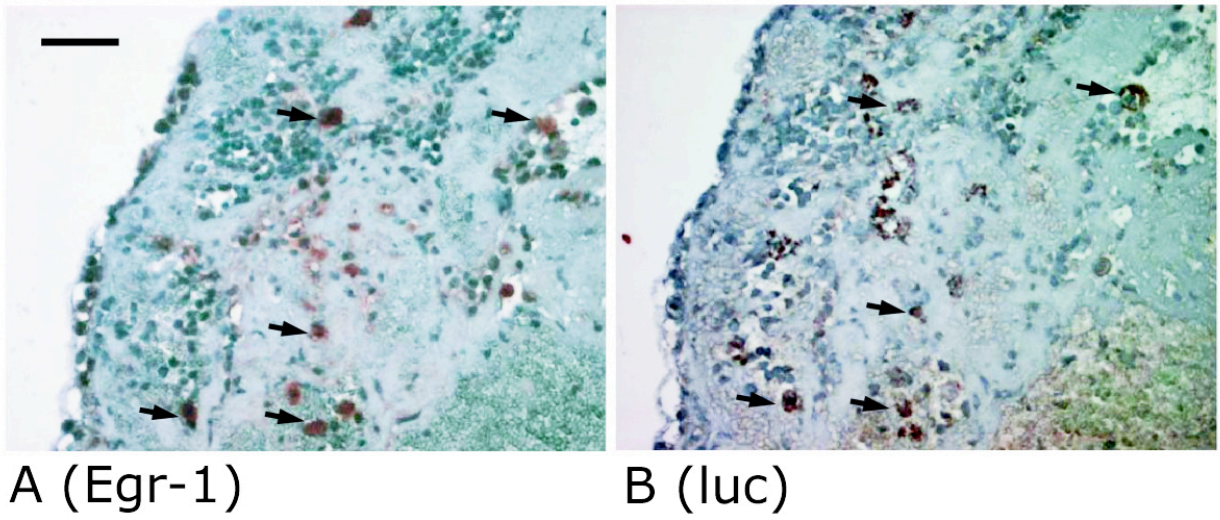

Figure 14: Immunohistochemical analyses of Egr-1 driven luciferase expression in regenerating liver

Egr1-luc mice 4 – 8 weeks of age were subject to one-third liver hepatectomy as described. 48 h after surgery mice were sacrificed, liver tissue fixed in paraformaldehyde and stained for luciferase. Tissue next to the site of surgery (rim lower left corner in both images) is shown and cells staining positive for Egr-1 (A) as well as luciferase (B) appear as clusters with lilac staining (arrows; scale bar: 50 µm).

3.5.2 Quantitative Egr-1 levels in liver regeneration

To obtain a quantitative view on Egr-1 levels in liver regeneration, animals were sacrificed 12 h or 48 h after surgery and liver tissue homogenized for mRNA and protein quantification of Egr-1 and luciferase, respectively (Fig 15). 12 h after surgery, protein levels of Egr-1 were six times higher compared to the sham operated group (Fig 15B). For luciferase, the mRNA level was not detectable in the sham operated group, whereas in hepatectomized animals a strong signal was found. Analyzing protein levels 48 h after surgery, an increased signal was found for both Egr-1 and luciferase (Fig 15A). Compared to Egr-1 this increase was considerably more pronounced for luciferase (Fig 15), which can be explained by the fact that luciferase protein has a considerably longer intracellular half life of 3 hours, (Thompson, Hayes et al. 1991) than the Egr-1 protein, which is degraded more rapidly and has a half live of less than 2 hours, generally between 30 min to 1 hour (Waters, Hancock et al. 1990).

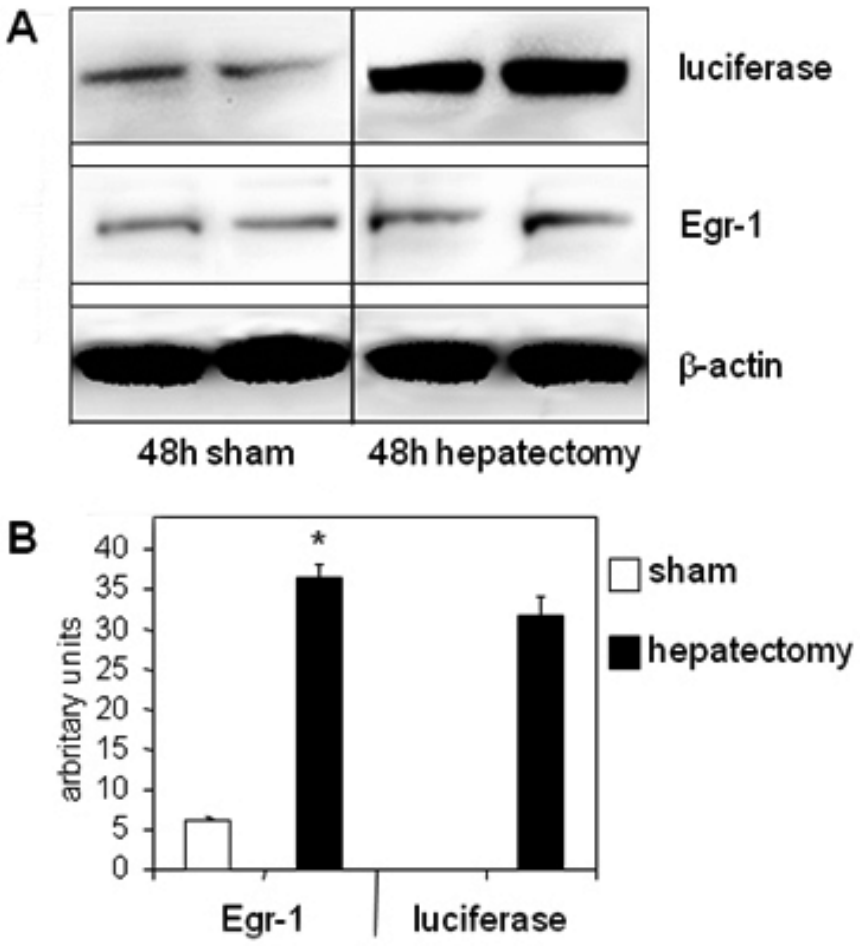

Figure 15: mRNA and protein levels of Egr-1 and luciferase after partial hepatectomy

Egr-1-Luc mice were subject to one third hepatectomy or sham operation, sacrificed 48h (A) or 12h (B) after surgery and liver tissue subject to mRNA analyses by qRT-PCR (B) or Western blotting analyzing protein levels of Egr-1 and luciferase (A).

(A) Representative Western blots showing the protein levels of Egr-1, luciferase and β-actin to confirm equal loading for hepatectomized (right panel) or sham operated animals (left panel), respectively; data from two representative animals per treatment are shown.

(B) mRNA levels of Egr-1 and luciferase, respectively (average relative mRNA levels relative to 18S rRNA levels); mRNA levels of luciferase in sham operated animals was below the detection limit. n=4; * $p<0.05$ sham vs. hepatectomy (U-test, Mann-Whitney)

3.6 Egr-1 activation in wound healing

Using in vivo BLI, I monitored the activity of the Egr-1 promoter in Egr-1-luc mice immediately after the infliction of a punch wound on the right ear. For quantification we used defined ROI's. The Egr-1 activity showed a major increase in the immediate vicinity of the wound, while more distant areas did not show any difference compared to the control (Fig 16A). Placing a ROI over the area surrounding the wound, a >12-fold increased BLI signal was found 24 h after infliction of the wound when compared to an equal sized ROI on the adjacent control ear (Fig 16B).

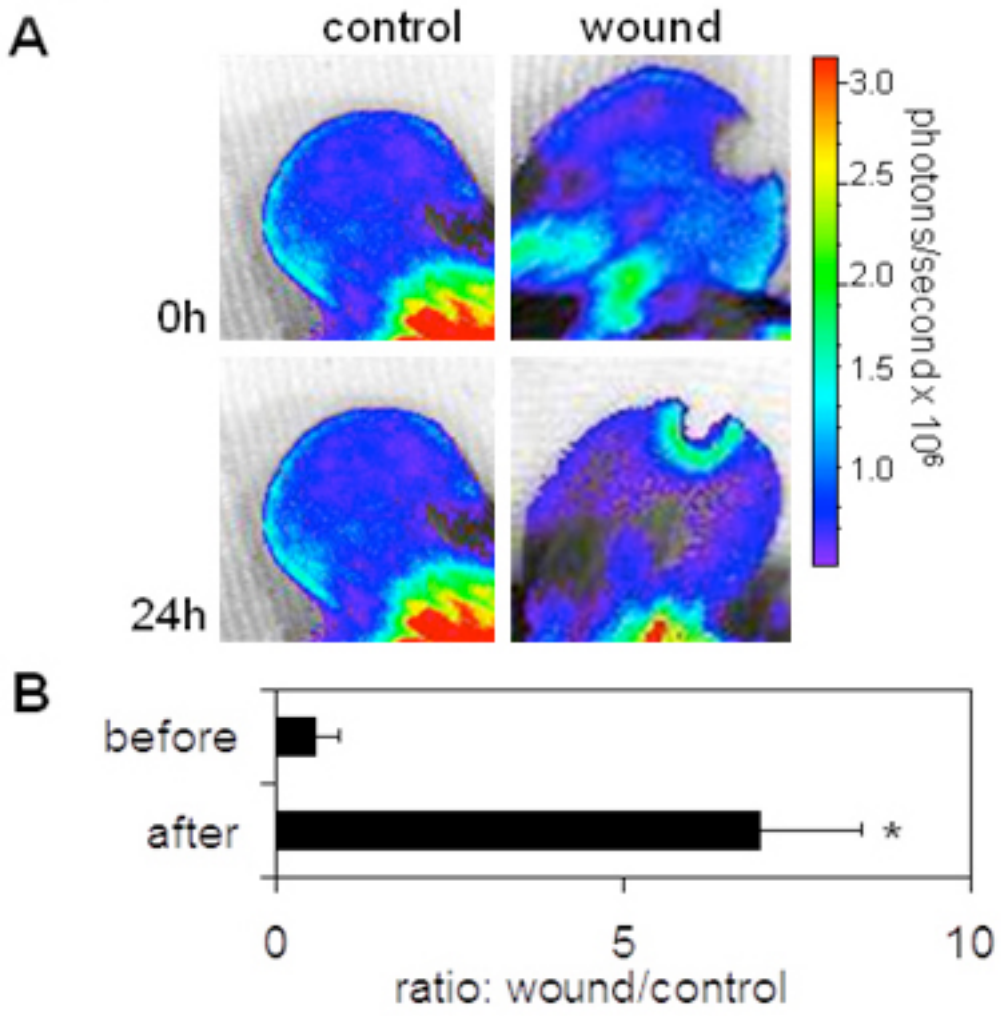

Figure 16: In vivo bioluminescence imaging of the ear-wound

In Egr-1-luc mice between the ages of 4 – 8 weeks an ear wound was inflicted in one ear. 0 h and 24 h after infliction animals were subject to BLI. Luciferase signal was collected for 2 min from the wounded ear or the control ear.

(**A**) Color coded BLI image overlaid onto a reflected light image from the control ear (left) or wounded ear (right) immediately (top row) or 24 h (bottom row) after wound infliction.

(**B)** Quantitative luciferase signals from ROI's placed over the wound site or an equal sized ROI at the control ear immediately after the wound infliction (before) and 24 h thereafter (after); n=3; * $p<0.05$ control vs. wound (U-test, Mann-Whitney)

4 Discussion

The data collected in this study on both, Egr-1 and luciferase, is in line with previously published data on Egr-1. Data of all end-point and *in vitro* studies are in accordance with *in vivo* data and studies about protein kinetics over time. In synopsis, the results strongly support the proper functioning of this transgenic Egr-1-luc murine model. The data supports the functionality of this model to observe the *in-vivo* Egr-1 promoter activity over time in the same animal.

4.1 The Egr-1-luc murine model

The Egr-1-luc murine model has been characterized as a novel model allowing the *in vivo* study of Egr-1 promoter activity and therefore protein expression and kinetics over time. The BLI of adult mice showed the highest signal intensities in the lip, snout, ears and paw regions (Fig. 9). It can be postulated that these anatomical regions are still undergoing more developmental changes, such as the continued growth of teeth, of tendons in the extremities or of outer ear tissue, than other areas of the body. Indeed, Egr-1 has been previously identified to be involved in periodontal regeneration (Ivanovski, Lichanska et al. 2007) and embryonic tendon formation (Lejard, Blais et al. 2011). While Egr-1 has to be determined further, an involvement of Egr-1 in the continued growth of the outer ear tissue in 4-month-old mice seems likely. My results show that a functional luciferases protein product is expressed as expected and the quantitative and qualitative measurement of the luciferase luminescence yields satisfactory results in the Egr-1-luc transgenic mouse model. In the remaining fur covered regions of the animal, little to no luciferase signal was detected. Due to the fact that this transgenic model was constructed of C57BL6 background, this absence of

signal could be in part due to quenching effects. The mouse lineage used is covered by a thick dark fur, which could obliterate the detection of photons emitted from underlying cells. To account for this possibility and to minimize the possibility of quenching effects, BLI and quantitative measurements of luciferases signals for all experiments are designed to be carried out only on areas covered by no or very little fur. In addition to the *in vivo* experiments, the luminescence measurements of SMC cultures proved that primary cells from the transgenic Egr-1-luc mouse model are also suitable for *in vitro* studies.

4.2 Cell culture studies

The results of luciferase activity *in vitro* obtained in the SMC cultures, demonstrate the Egr-1 promoter activity in proliferating *in vitro* cultures of SMC and point to the functions of Egr-1 in vasculature (J.I.Pagel 2010) These results are in line with Egr-1 activities described in the literature for SMC (Fahmy and Khachigian 2007). As the major aim of this work was to monitor Egr-1 activity *in vivo*, I pursued the *in vitro* cultures not further.

4.3 Developmental studies

It has previously been shown that tumor necrosis factor α (TNF α) and VEGF have both induced Egr-1 expression in endothelial cells (Mechtcheriakova, Schabbauer et al. 2001). In our developmental experiments, Egr-1 promoter activity was observed to be highest at day 7 after birth, the earliest time point measured and to decrease rapidly in the following days until reaching a much lower baseline level at day 21. VEGFR-2 promoter controlled luciferase expression was analyzed in a similar way in neonatal mice (Zhang, Fang et al. 2004): At the earliest time point measured in those experiments at 2 weeks after birth highest

luciferase activity was found throughout the entire body, whereas in mice 6 weeks of age the signal was about 100-fold reduced and remained constant for up to 15 weeks after birth. Due to our results, it is likely that there appears to be a spatial and temporal correlation between VEGF and Egr-1 activity during neonatal development. In our study, Egr-1 promoter controlled luciferase activity reached baseline levels already three weeks after birth indicating a faster decrease then for VEGFR-2. *In vitro* studies showed the interconnection of VEGF and Egr-1, as in endothelial cells VEGF stimulation led to initially high Egr-1 levels (Cao, Mahendran et al. 1993). Besides VEGF, other growth factors up-regulated in neonatal organism, like FGF-1 and -2 can activate Egr-1 (Damon, Lange et al. 1997), whereas the decrease in Egr-1 activity can be explained by the negative feedback loop of Egr-1, which can bind to the EBS sites located within its own promoter region (Cao, Mahendran et al. 1993) leading to a 'fine tuning' of its activity. Apparently Egr-1 is involved in the cell proliferation process during postnatal growth and decreases in the adult. The activity of Egr-1 is on a high level almost all over the entire ventral anatomy of the neonatal mouse and decreases - seemingly simultaneous to the growth rate - until reaching a baseline activity when mice are fully grown and cell proliferation reaches a relatively low baseline value. During this stage, the only significant Egr-1 activity was observed at the paws, snout, ears, and tail, which is in line with observation measuring VEGFR-2 promoter driven luciferase (Zhang, Fang et al. 2004). It still has to be determined which specific processes are taking place on these sites of high Egr-1 promoter activity relative to the rest of the body.

The pattern of Egr-1 promoter activity (developing limbs, central nervous system, mandibles) is at least in part similar to the pattern of ERK signaling during embryogenesis, were major sites of ERK activity were observed, besides others, in limb buds, the forebrain and fronto-nasal processes (Corson, Yamanaka et al. 2003). This expression pattern observed points at the interconnection between ERK and Egr-1 signaling. The data clearly demonstrates that Egr-1 is highly up regulated

throughout the body during neonatal development, where I observed maximal activity at day seven after birth, the earliest time point measured. Similar observations were made with transgenic mice expressing VEGF promoter driven luciferase in neonatal mice (Faley, Takahashi et al. 2007). Also here maximal activity was observed one week after birth followed by a continuous decline in activity further on. When stimulating endothelial cells *in vitro* with VEGF, TNFα or thrombin, activation of Egr-1 was observed (Suehiro, Hamakubo et al. 2010). I supplemented our developmental experiments with immunohistochemical analyses of several tissues of the mice embryo to further validate the data obtained from BLI further. Here, the luciferase and Egr-1 staining of hind limb and masticatory tissues showed that protein expression for both were in accordance with the BLI data.

4.4 Liver regenerating studies

The involvement of Egr-1 in liver regeneration was first described by Müller and colleagues (Mueller, Broering et al. 2002), and Egr-1 knockout mice showed significantly delayed liver regeneration after hepatectomy (Liao, Shikapwashya et al. 2004). The importance of Egr-1 expression in liver injury has also been described in ethanol induced fatty liver, where Egr-1 promoted TNFα expression (McMullen, Pritchard et al. 2005). It was previously shown, that liver regeneration after partial hepatectomy is decreased in Egr-1 deficient mice because of impaired progression of mitosis, due to missing Egr-1–regulated expression of cell division cycle protein 20 homolog (Cdc20) (Liao, Shikapwashya et al. 2004). In our liver regeneration experiment, we have demonstrated that Egr-1 promoter driven luciferase expression was induced at the early stages of liver regeneration. After only 12 hours from surgery mRNA levels of luciferase and Egr-1 were already strongly elevated, which is in line with results obtained in rats (Mueller, Broering et al. 2002). Interestingly, luciferase

activity and protein level were both elevated at 48 h after surgery.

During the regeneration of liver tissue, quiescent liver cells reenter the cell cycle and divide until the original liver mass is restored (Fausto, Campbell et al. 2006). Besides the profound induction of proliferation, partial hepatectomy leads to local hypoxia in the ischemic stump left after excision. This effect has been shown by the up-regulation of hypoxia inducible factor 1 (HIF-1) (Maeno, Ono et al. 2005), which is closely associated with the presence of tissue hypoxia. In those experiments it was observed that the levels of HIF-1α peaked at 24 h after surgery, whereas the peak levels of VEGF appeared only at later time points. Hence, the induction of Egr-1 after partial hepatectomy can, in addition to the stimulation of liver cells to proliferate, also be in part due to hypoxic conditions, an effect that has been described previously (Yan, Lu et al. 1999; Nishi, Nishi et al. 2002; Liao, Shikapwashya et al. 2004). This same effect has also already been described for macrophages *in vitro*, where hypoxia induced Egr-1 expression occurred after hypoxic treatment (Elbarghati, Murdoch et al. 2008).

Even though the major Egr-1 promoter activity was observed in the area of the initial surgery wound, which is mainly due to the wound healing processes and hypoxic conditions, some elevated activity was visible at the edges of the remaining lobes suggesting the onset tissue regeneration by the means of cell division and proliferation. These results support the reported findings of impaired mitosis in Egr-1 deficient mice (Liao, Shikapwashya et al. 2004) and evidence that Egr-1 is not only induced within the healing process, but also during other processes where cell division and proliferation are involved.

4.5 Wound healing studies

At the early stages of wound healing, an inflammatory response followed by re-epithelialization of the wound area and establishment of granulation tissue with accompanying neovascularization occurs (Clark 1993). Due to the interaction of Egr-1 and inflammatory parameters, like TNFα (McMullen, Pritchard et al. 2005; Rockel, Bernier et al. 2009; Rockel, Grol et al. 2009) and others, Egr-1 is involved in the wound healing process. In Egr-1 deficient mice wound healing, immune response and the influx of inflammatory cells was significantly reduced, whereas Egr-1 overexpression led in turn to exuberant tissue repair and enhanced collagen production (Wu, Melichian et al. 2009). The wound healing experiments are thus extremely suitable to show the functionality of the Egr-1-luc transgenic mouse model. The data of the ear wound experiment confirms *in vivo* that Egr-1 indeed is playing a major role in the inflammatory response and the wound healing process. Its activity in the tissue surrounding the immediate wound area was found to be increased by >12-fold whereas Egr-1 expression in tissue more distant to the wound remained unaltered.

5 Summary and Outlook

5.1 Summary

In summary, the present study shows that the observation of luciferase activity, which is congruent with Egr-1-promoter activity over time in the living transgenic Egr-1-luc animal model allows gaining a view of the spatial expression pattern of luc and their changes over time *in vivo*. The results confirm the ubiquitous role of Egr-1 in proliferation, regeneration, wound healing and development. The present study monitored the Egr-1 activation pattern over time in transgenic mice expressing Egr-1 promoter driven luciferase and showed the spatial expression pattern and their time dependent change *in vivo*. This transgenic mouse provides a convenient model for studying Egr-1 expression during neonatal development and wound healing at areas were the fur of mice with C57/bl6 background does not interfere with BLI imaging. In neonatal mice, high overall Egr-1 promoter activity was observed, which reached basal levels three weeks after birth with residual activity remaining at snout, ears and paws. In wound healing, Egr-1 promoter activity was highly up regulated at the site of injury.

Monitoring Egr-1 activity within internal organs, such as in the liver regeneration model presented, was only possible by endpoint measurements with animals having an opened body cavity. Here it was observed, that Egr-1 promoter activity and Egr-1 mRNA levels were increased in the regenerating liver after partial hepatectomy.

In summary, this mouse model allows real time *in vivo* imaging of Egr-1 promoter activity during development, tissue regeneration and wound healing *in vivo* and *in vitro* measurement of Egr-1 promoter activity in SMC cell cultures.

To further improve its usability for BLI, crossbreeding into hairless mice will result in a further improvement of its sensitivity by decreasing

quenching effects of the fur. Moreover, BLI will then offer a useful tool for monitoring the tissue-specific effects of pharmaceutical drugs over time *in vivo*, too. This can be especially useful for the development of chemotherapeutic agents binding to certain cancer-specific proteins for example.

5.2 Outlook

Due to the advances of genetic engineering in organisms, the use of luciferase reporters became a useful monitoring tool to a wide range of applications and allows the real-time *in vivo* measurement of biologic processes. Since dynamic changes over time cannot be examined by end-point measurements, studying Egr-1 activity within the living organism will aid to gain new information on *in vivo* Egr-1 gene activation. One of the major advantages, which the use of non invasive measurements using luciferase reporters offer, is that biological changes can be observed in the same animals over a period of time without the absolute need to sacrifice the animals.

5.3 Zusammenfassung

Zusammenfassend zeigt die vorliegende Arbeit, dass das Egr-1-luc Tiermodell geeignet ist räumliche Egr-1 Expressionsmuster über eine Zeitspanne hinweg am lebenden Organismus *in vivo* qualitativ und quantitativ zu beobachten. Die Ergebnisse bestätigen die allgegenwärtige Rolle von Egr-1 bei der Proliferation, Regeneration, Wundheilung und Entwicklung. Diese Arbeit verfolgte das Egr-1 Aktivierungsmuster in transgenen Mäusen mittels der von dem Egr-1 Promoter kontrollierten Luciferase über verschiedene Zeitspannen hinweg und zeigt das räumliche Expressionsmuster und dessen Änderung im Zeitverlauf *in vivo*. Diese transgene Egr-luc Maus ist somit ein geeignetes Modell um die Egr-1-Expression während der Entwicklung von neugeborenen Tiere und der Wundheilung an Bereichen, an denen das Fell der Tiere mit C57/BL6 Hintergrund nicht die BLI Bildgebung stört, zu beobachten. In neugeborenen Mäusen (7. Lebenstag) wurde eine insgesamt hohe Egr-1-Promotor-Aktivität beobachtet, welche bis zum 21. Tag nach Geburt kontinuierlich auf ein Basallevel mit einer Restaktivität an Schnauze, Ohren und Pfoten abnahm. Bei der Wundheilung wurde eine stark hochregulierte Egr-1-Promotor-Aktivität in der unmittelbaren Umgebung der Verletzung nach 24 Stunden gezeigt. Die Beobachtung der Egr-1-Aktivität an der Oberfläche innerer Organe, wie in dem hier vorgestellten Modell der Leberregeneration, war lediglich durch End-Point-Messungen möglich, da die Körperhöhle der Tiere hierzu eröffnet werden musste. In diesem Experiment wurde beobachtet, dass die Egr-1-Promotor-Aktivität und die Egr-1 mRNA-Spiegel in der regenerierenden Leber nach partieller Hepatektomie erhöht waren. Zusammenfassend erlaubt die Egr-luc Maus eine *in vivo* Bildgebung der Egr-1-Promotor-Aktivität während der Entwicklung, der Geweberegeneration und Wundheilung in Echtzeit und die *in vitro* Messung der Egr-1 Promoter Aktivität in SMC Zellkulturen. Zu einer weiteren Verbesserung dieses Modells für BLI könnten Kreuzungen mit haarlosen Mäusen führen und die Sensitivität dieses Modells für BLI -

durch die Verminderung von Signalauslöschung durch das Fell - weiter verbessern. Es ist weiterhin zu erwarten, dass BLI dann auch zur *in vivo* Beobachtung der gewebsspezifischen Wirkungen von Pharmazeutika im Zeitverlauf eingesetzt werden könnte. Dies kann zum Beispiel bei der Entwicklung von Pharmazeutika in der Chemotherapie, die an bestimmte Karzinom-spezifische Proteine binden, besonders nützlich sein.

6 Appendix

6.1 Abbreviations

ALI	acute lung injury
AMP	adenosine mono phosphate
AP1	activated protein-1 responsive element
ATP	adenosine tri phosphate
BLI	body luminescence imaging
bp	base pair
cAMP	cyclic adenosine mono phosphate
CBP	cAMP response element binding protein
CCD	cooled charge-coupled device
Cdc20	cell division cycle protein 20
cDNA	complementary DNA
CMF	chicken embryo fibroblasts
CMV	cytomegalovirus
CoA	coenzyme A
COPD	chronic obstructive pulmonary disease
C-terminus	carboxy-terminus
DTT	dithiothreitol
DNA	deoxyribonucleic acid
EBS	Egr-1 binding sequence

EDTA	ethylene diamine tetra-acetic acid
Egr	early growth response
ERK	extracellular regulated kinase
FCS	fetal calf serum
FGF	fibroblast growth factor
Fig.	figure
g	gram
g	standard gravity (=9,806 $m/s^{2)}$
h	hour
HCl	hydrochloric acid
HIF	hypoxia inducible factor
HIV	human immunodeficiency virus
HRP	horseradish peroxidase
HSV	herpes simplex virus
i.p.	intra-peritoneal
ICAM	intercellular adhesion molecule
Il	inter-leucine
kDa	kilo Dalton
LAR	luciferases assay reagent
LCI	luciferase complementation imaging
LED	light-emitting diode
Luc	luciferases

MHV	mouse hepatitis virus
min	minute
mm	millimeter
MMP	matrix metalloproteinase
mRNA	messenger ribonucleic acid
n	number
Nab	NGFI-A binding protein
N-terminus	amino-terminus
nm	nanometer
NGF	nerve growth factor
NGFI-A	nerve growth factor inducible A
NLS	nuclear localization signal
N-terminus	Amino-terminus
PBS	phosphate-buffered saline
PCR	polymerase chain reaction
PDGF	platelet derived growth factor
PFA	paraformaldehyde
qRT-PCR	quantitative real time polymerase chain reaction
RLU	relative light units
RNA	ribonucleic acid
ROI	regions of interest
Rpm	rounds per minute

rRNA	ribosomal RNA
RT-PCR	real-time polymerase chain reaction
sec	second
SMC	smooth muscle cells
SRE	serum response element
TBS	tris buffered saline
TNFα	tumor necrosis factor α
TRE	thiophorbolester responsive element
tRNA	total ribonucleic acid
UV	ultraviolet
VEGF	vascular endothelial growth factor
VEGFR	vascular endothelial growth factor receptor
ZENK	zif268, egr-1, NGFI-A, krox24
Zif	zinc finger

6.2 Publications

This dissertation was published in parts:

Dussmann P, Pagel JI, Vogel S, Magnusson T, Zimmermann R, Wagner E, Schaper W, Ogris M, Deindl E, 2011, Live in vivo imaging of Egr-1 promoter activity during neonatal development, liver regeneration and wound healing, BMC Dev Biol. 2011 May 20;11:28, PMID: 21595990[PubMed - in process] PMCID: PMC3120781 (Dussmann, Pagel et al. 2011)

6.3 Declaration: **Eidesstattliche Versicherung**

Dußmann, Philipp Sebastian Wilhelm Lukas

Name, Vorname

Ich erkläre hiermit an Eides statt,

dass ich die vorliegende Dissertation mit dem Thema

selbständig verfasst, mich außer der angegebenen keiner weiteren Hilfsmittel bedient und alle Erkenntnisse, die aus dem Schrifttum ganz oder annähernd übernommen sind, als solche kenntlich gemacht und nach ihrer Herkunft unter Bezeichnung der Fundstelle einzeln nachgewiesen habe.

Ich erkläre des Weiteren, dass die hier vorgelegte Dissertation nicht in gleicher oder in ähnlicher Form bei einer anderen Stelle zur Erlangung eines akademischen Grades eingereicht wurde.

München, 25.02.2016

Ort, Datum

Unterschrift Doktorandin/Doktorand

7 References

Abdel-Malak, N. A., M. Mofarrahi, et al. (2009). "Early growth response-1 regulates angiopoietin-1-induced endothelial cell proliferation, migration, and differentiation." Arterioscler Thromb Vasc Biol **29**(2): 209-216.

Barancik, M., P. Htun, et al. (2000). "Inhibition of the cardiac p38-MAPK pathway by SB203580 delays ischemic cell death." J Cardiovasc Pharmacol **35**(3): 474-483.

Bedadala, G. R., J. R. Palem, et al. (2011). "Lytic HSV-1 infection induces the multifunctional transcription factor Early Growth Response-1 (EGR-1) in rabbit corneal cells." Virol J **8**: 262.

Blaschke, F., D. Bruemmer, et al. (2004). "Egr-1 is a major vascular pathogenic transcription factor in atherosclerosis and restenosis." Rev Endocr Metab Disord **5**(3): 249-254.

Brock, M., G. Jouvion, et al. (2008). "Bioluminescent Aspergillus fumigatus, a new tool for drug efficiency testing and in vivo monitoring of invasive aspergillosis." Appl Environ Microbiol **74**(22): 7023-7035.

Cai, Y., Y. Liu, et al. (2006). "Induction of transcription factor Egr-1 gene expression in astrocytoma cells by Murine coronavirus infection." Virology **355**(2): 152-163.

Cao, X., R. Mahendran, et al. (1993). "Detection and characterization of cellular EGR-1 binding to its recognition site." J Biol Chem **268**(23): 16949-16957.

Cao, X. M., R. A. Koski, et al. (1990). "Identification and characterization of the Egr-1 gene product, a DNA-binding zinc finger protein induced by differentiation and growth signals." Mol Cell Biol **10**(5): 1931-1939.

Cho, S. J., M. J. Kang, et al. (2006). "Role of early growth response-1 (Egr-1) in interleukin-13-induced inflammation and remodeling." J Biol Chem **281**(12): 8161-8168.

Chomczynski, P. and N. Sacchi (1987). "Single-step method of RNA isolation by acid guanidinium thiocyanate-phenol-chloroform extraction." Anal Biochem **162**(1): 156-159.

Christy, B. and D. Nathans (1989). "DNA binding site of the growth factor-inducible protein Zif268." Proc Natl Acad Sci U S A **86**(22): 8737-8741.

Clark, R. A. (1993). "Biology of dermal wound repair." Dermatol Clin **11**(4): 647-666.

Contag, C. H., S. D. Spilman, et al. (1997). "Visualizing gene expression in living mammals using a bioluminescent reporter." Photochem Photobiol **66**(4): 523-531.

Conti, E., N. P. Franks, et al. (1996). "Crystal structure of firefly luciferase throws light on a superfamily of adenylate-forming enzymes." Structure **4**(3): 287-298.

Copland, I. B., B. P. Kavanagh, et al. (2003). "Early changes in lung gene expression due to high tidal volume." Am J Respir Crit Care Med **168**(9): 1051-1059.

Corson, L. B., Y. Yamanaka, et al. (2003). "Spatial and temporal patterns of ERK signaling during mouse embryogenesis." Development **130**(19): 4527-4537.

Damon, D. H., D. L. Lange, et al. (1997). "In vitro and in vivo vascular actions of basic fibroblast growth factor (bFGF) in normotensive and spontaneously hypertensive rats." J Cardiovasc Pharmacol **30**(3): 278-284.

Datta, R., N. Taneja, et al. (1993). "Reactive oxygen intermediates target CC(A/T)6GG sequences to mediate activation of the early growth response 1 transcription factor gene by ionizing radiation." Proc Natl Acad Sci U S A **90**(6): 2419-2422.

de Wet, J. R., K. V. Wood, et al. (1987). "Firefly luciferase gene: structure and expression in mammalian cells." Mol Cell Biol **7**(2): 725-737.

Deuschle, U., R. Pepperkok, et al. (1989). "Regulated expression of foreign genes in mammalian cells under the control of coliphage T3 RNA polymerase and lac repressor." Proc Natl Acad Sci U S A **86**(14): 5400-5404.

Dumollard, R., P. Marangos, et al. (2004). "Sperm-triggered [Ca2+] oscillations and Ca2+ homeostasis in the mouse egg have an absolute requirement for mitochondrial ATP production." Development **131**(13): 3057-3067.

Dussmann, P., J. I. Pagel, et al. (2011). "Live in vivo imaging of Egr-1 promoter activity during neonatal development, liver regeneration and wound healing." BMC Dev Biol **11**: 28.

Elbarghati, L., C. Murdoch, et al. (2008). "Effects of hypoxia on transcription factor expression in human monocytes and macrophages." Immunobiology **213**(9-10): 899-908.

Elrod-Erickson, M., M. A. Rould, et al. (1996). "Zif268 protein-DNA complex refined at 1.6 A: a model system for understanding zinc finger-DNA interactions." Structure **4**(10): 1171-1180.

Fahmy, R. G. and L. M. Khachigian (2007). "Suppression of growth factor expression and human vascular smooth muscle cell growth by small interfering RNA targeting EGR-1." J Cell Biochem **100**(6): 1526-1535.

Faley, S. L., K. Takahashi, et al. (2007). "Bioluminescence imaging of vascular endothelial growth factor promoter activity in murine mammary tumorigenesis." Mol Imaging **6**(5): 331-339.

Fan, Y., W. Zou, et al. (2011). "Activation of Egr-1 expression in astrocytes by HIV-1 Tat: new insights into astrocyte-mediated Tat neurotoxicity." J Neuroimmune Pharmacol **6**(1): 121-129.

Fausto, N., J. S. Campbell, et al. (2006). "Liver regeneration." Hepatology **43**(2 Suppl 1): S45-53.

Forsdyke, D. R. (1985). "cDNA cloning of mRNAS which increase rapidly in human lymphocytes cultured with concanavalin-A and cycloheximide." Biochem Biophys Res Commun **129**(3): 619-625.

Foucault, M. L., L. Thomas, et al. (2010). "In vivo bioluminescence imaging for the study of intestinal colonization by Escherichia coli in mice." Appl Environ Microbiol **76**(1): 264-274.

Gashler, A. and V. P. Sukhatme (1995). "Early growth response protein 1 (Egr-1): prototype of a zinc-finger family of transcription factors." Prog Nucleic Acid Res Mol Biol **50**: 191-224.

Gashler, A. L., S. Swaminathan, et al. (1993). "A novel repression module, an extensive activation domain, and a bipartite nuclear localization signal defined in the immediate-early transcription factor Egr-1." Mol Cell Biol **13**(8): 4556-4571.

Gius, D., X. M. Cao, et al. (1990). "Transcriptional activation and repression by Fos are independent functions: the C terminus represses immediate-early gene expression via CArG elements." Mol Cell Biol **10**(8): 4243-4255.

Gokey, N. G., C. Lopez-Anido, et al. (2011). "Early growth response 1 (Egr-1) regulates cholesterol biosynthetic gene expression." J Biol Chem.

Gould, S. G., G. A. Keller, et al. (1987). "Identification of a peroxisomal targeting signal at the carboxy terminus of firefly luciferase." J Cell Biol **105**(6 Pt 2): 2923-2931.

Greer, L. F., 3rd and A. A. Szalay (2002). "Imaging of light emission from the expression of luciferases in living cells and organisms: a review." Luminescence **17**(1): 43-74.

Haas, T. L., D. Stitelman, et al. (1999). "Egr-1 mediates extracellular matrix-driven transcription of membrane type 1 matrix metalloproteinase in endothelium." J Biol Chem **274**(32): 22679-22685.

Hasan, M. Y., W. B. Alshuaib, et al. (2003). "Effects of alpha-tocopherol on diabetes-induced alterations of synaptic transmission and contractile features in murine dorsiflexor muscle." Endocr Res **29**(4): 419-428.

Hasan, R. N., S. Phukan, et al. (2003). "Differential regulation of early growth response gene-1 expression by insulin and glucose in vascular endothelial cells." Arterioscler Thromb Vasc Biol **23**(6): 988-993.

Ivanovski, S., A. M. Lichanska, et al. (2007). "Gene expression profiling of cells involved in periodontal regeneration." Tissue Eng **13**(2): 393-404.

J.I.Pagel, E. D. (2010). "Concepts of Egr-1 Activation - A Hub for Signal Transduction Cascades." Current Signal Transduction Therapy(2): 149 - 160.

James, A. B., A. M. Conway, et al. (2006). "Regulation of the neuronal proteasome by Zif268 (Egr1)." J Neurosci **26**(5): 1624-1634.

Jawhara, S. and S. Mordon (2004). "In vivo imaging of bioluminescent Escherichia coli in a cutaneous wound infection model for evaluation of an antibiotic therapy." Antimicrob Agents Chemother **48**(9): 3436-3441.

Jones, M. W., M. L. Errington, et al. (2001). "A requirement for the immediate early gene Zif268 in the expression of late LTP and long-term memories." Nat Neurosci **4**(3): 289-296.

Keeton, A. B., K. D. Bortoff, et al. (2003). "Insulin-regulated expression of Egr-1 and Krox20: dependence on ERK1/2 and interaction with p38 and PI3-kinase pathways." Endocrinology **144**(12): 5402-5410.

Kharbanda, S., T. Nakamura, et al. (1991). "Expression of the early growth response 1 and 2 zinc finger genes during induction of monocytic differentiation." J Clin Invest **88**(2): 571-577.

Ko, S. W., K. I. Vadakkan, et al. (2005). "Selective contribution of Egr1 (zif/268) to persistent inflammatory pain." J Pain **6**(1): 12-20.

Kramer, B., A. Meichle, et al. (1994). "Characterization of an Krox-24/Egr-1-responsive element in the human tumor necrosis factor promoter." Biochim Biophys Acta **1219**(2): 413-421.

Kumbrink, J., M. Gerlinger, et al. (2005). "Egr-1 induces the expression of its corepressor nab2 by activation of the nab2 promoter thereby establishing a negative feedback loop." J Biol Chem **280**(52): 42785-42793.

Kumbrink, J., K. H. Kirsch, et al. (2010). "EGR1, EGR2, and EGR3 activate the expression of their coregulator NAB2 establishing a negative feedback loop in cells of neuroectodermal and epithelial origin." J Cell Biochem **111**(1): 207-217.

Lee, C. G., S. J. Cho, et al. (2004). "Early growth response gene 1-mediated apoptosis is essential for transforming growth factor beta1-induced pulmonary fibrosis." J Exp Med **200**(3): 377-389.

Lee, S. L., Y. Sadovsky, et al. (1996). "Luteinizing hormone deficiency and female infertility in mice lacking the transcription factor NGFI-A (Egr-1)." Science **273**(5279): 1219-1221.

Lee, S. L., L. C. Tourtellotte, et al. (1995). "Growth and differentiation proceeds normally in cells deficient in the immediate early gene NGFI-A." J Biol Chem **270**(17): 9971-9977.

Lee, S. L., Y. Wang, et al. (1996). "Unimpaired macrophage differentiation and activation in mice lacking the zinc finger transplantation factor NGFI-A (EGR1)." Mol Cell Biol **16**(8): 4566-4572.

Lejard, V., F. Blais, et al. (2011). "EGR1 and EGR2 involvement in vertebrate tendon differentiation." J Biol Chem **286**(7): 5855-5867.

Lemaire, P., O. Revelant, et al. (1988). "Two mouse genes encoding potential transcription factors with identical DNA-binding domains are activated by growth factors in cultured cells." Proc Natl Acad Sci U S A **85**(13): 4691-4695.

Li, C. J., W. Ning, et al. (2007). "MAPK pathway mediates EGR-1-HSP70-dependent cigarette smoke-induced chemokine production." Am J Physiol Lung Cell Mol Physiol **292**(5): L1297-1303.

Liao, Y., O. N. Shikapwashya, et al. (2004). "Delayed hepatocellular mitotic progression and impaired liver regeneration in early growth response-1-deficient mice." J Biol Chem **279**(41): 43107-43116.

Lim, R. W., B. C. Varnum, et al. (1987). "Cloning of tetradecanoyl phorbol ester-induced 'primary response' sequences and their expression in density-arrested Swiss 3T3 cells and a TPA non-proliferative variant." Oncogene **1**(3): 263-270.

Lu, Y., T. Li, et al. (2011). "Early Growth Response 1 (Egr-1) Regulates Phosphorylation of Microtubule-associated Protein Tau in Mammalian Brain." J Biol Chem **286**(23): 20569-20581.

Luker, G. D., J. P. Bardill, et al. (2002). "Noninvasive bioluminescence imaging of herpes simplex virus type 1 infection and therapy in living mice." J Virol **76**(23): 12149-12161.

Luker, K. E. and D. Piwnica-Worms (2004). "Optimizing luciferase protein fragment complementation for bioluminescent imaging of protein-protein interactions in live cells and animals." Methods Enzymol **385**: 349-360.

Maddox, S. A., M. S. Monsey, et al. (2011). "Early growth response gene 1 (Egr-1) is required for new and reactivated fear memories in the lateral amygdala." Learn Mem **18**(1): 24-38.

Maeno, H., T. Ono, et al. (2005). "Expression of hypoxia inducible factor-1alpha during liver regeneration induced by partial hepatectomy in rats." Liver Int **25**(5): 1002-1009.
Mahalingam, D., A. Natoni, et al. (2010). "Early growth response-1 is a regulator of DR5-induced apoptosis in colon cancer cells." Br J Cancer **102**(4): 754-764.
Maltzman, J. S., J. A. Carmen, et al. (1996). "Transcriptional regulation of the Icam-1 gene in antigen receptor- and phorbol ester-stimulated B lymphocytes: role for transcription factor EGR1." J Exp Med **183**(4): 1747-1759.
Matheny, C., M. L. Day, et al. (1994). "The nuclear localization signal of NGFI-A is located within the zinc finger DNA binding domain." J Biol Chem **269**(11): 8176-8181.
McCaffrey, T. A., C. Fu, et al. (2000). "High-level expression of Egr-1 and Egr-1-inducible genes in mouse and human atherosclerosis." J Clin Invest **105**(5): 653-662.
McMahon, A. P., J. E. Champion, et al. (1990). "Developmental expression of the putative transcription factor Egr-1 suggests that Egr-1 and c-fos are coregulated in some tissues." Development **108**(2): 281-287.
McMahon, S. B. and J. G. Monroe (1996). "The role of early growth response gene 1 (egr-1) in regulation of the immune response." J Leukoc Biol **60**(2): 159-166.
McMullen, M. R., M. T. Pritchard, et al. (2005). "Early growth response-1 transcription factor is essential for ethanol-induced fatty liver injury in mice." Gastroenterology **128**(7): 2066-2076.
Mechtcheriakova, D., G. Schabbauer, et al. (2001). "Specificity, diversity, and convergence in VEGF and TNF-alpha signaling events leading to tissue factor up-regulation via EGR-1 in endothelial cells." FASEB J **15**(1): 230-242.
Mello, C. V., D. S. Vicario, et al. (1992). "Song presentation induces gene expression in the songbird forebrain." Proc Natl Acad Sci U S A **89**(15): 6818-6822.
Meyer, R. G., J. H. Kupper, et al. (2002). "Early growth response-1 gene (Egr-1) promoter induction by ionizing radiation in U87 malignant glioma cells in vitro." Eur J Biochem **269**(1): 337-346.
Milbrandt, J. (1987). "A nerve growth factor-induced gene encodes a possible transcriptional regulatory factor." Science **238**(4828): 797-799.
Mitchell, C. and H. Willenbring (2008). "A reproducible and well-tolerated method for 2/3 partial hepatectomy in mice." Nat Protoc **3**(7): 1167-1170.
Mueller, L., D. C. Broering, et al. (2002). "The induction of the immediate-early-genes Egr-1, PAI-1 and PRL-1 during liver regeneration in surgical models is related to increased portal flow." J Hepatol **37**(5): 606-612.
Ning, W., Y. Dong, et al. (2007). "Cigarette smoke stimulates matrix metalloproteinase-2 activity via EGR-1 in human lung fibroblasts." Am J Respir Cell Mol Biol **36**(4): 480-490.
Nishi, H., K. H. Nishi, et al. (2002). "Early Growth Response-1 gene mediates up-regulation of epidermal growth factor receptor expression during hypoxia." Cancer Res **62**(3): 827-834.
O'Donovan, K. J., E. P. Wilkens, et al. (1998). "Sequential expression of Egr-1 and Egr-3 in hippocampal granule cells following electroconvulsive stimulation." J Neurochem **70**(3): 1241-1248.
Ogris, M., R. C. Carlisle, et al. (2001). "Melittin enables efficient vesicular escape and enhanced nuclear access of nonviral gene delivery vectors." J Biol Chem **276**(50): 47550-47555.
Patwardhan, S., A. Gashler, et al. (1991). "EGR3, a novel member of the Egr family of genes encoding immediate-early transcription factors." Oncogene **6**(6): 917-928.
Paulmurugan, R., Y. Umezawa, et al. (2002). "Noninvasive imaging of protein-protein interactions in living subjects by using reporter protein complementation and reconstitution strategies." Proc Natl Acad Sci U S A **99**(24): 15608-15613.
Pavletich, N. P. and C. O. Pabo (1991). "Zinc finger-DNA recognition: crystal structure of a Zif268-DNA complex at 2.1 A." Science **252**(5007): 809-817.
Pelisek, J., S. Armeanu, et al. (2001). "Quiescence, cell viability, apoptosis and necrosis of smooth muscle cells using different growth inhibitors." Cell Prolif **34**(5): 305-320.

Ray, P., H. Pimenta, et al. (2002). "Noninvasive quantitative imaging of protein-protein interactions in living subjects." Proc Natl Acad Sci U S A **99**(5): 3105-3110.

Reumann, M. K., O. Strachna, et al. (2011). "Early growth response gene 1 regulates bone properties in mice." Calcif Tissue Int **89**(1): 1-9.

Reumann, M. K., O. Strachna, et al. (2011). "Loss of transcription factor early growth response gene 1 results in impaired endochondral bone repair." Bone.

Rice, B. W., M. D. Cable, et al. (2001). "In vivo imaging of light-emitting probes." J Biomed Opt **6**(4): 432-440.

Rockel, J. S., S. M. Bernier, et al. (2009). "Egr-1 inhibits the expression of extracellular matrix genes in chondrocytes by TNFalpha-induced MEK/ERK signalling." Arthritis Res Ther **11**(1): R8.

Rockel, J. S., M. Grol, et al. (2009). "Cyclic AMP regulates extracellular matrix gene expression and metabolism in cultured primary rat chondrocytes." Matrix Biol **28**(6): 354-364.

Rowe, L., E. Dikici, et al. (2009). "Engineering bioluminescent proteins: expanding their analytical potential." Anal Chem **81**(21): 8662-8668.

Russo, M. W., B. R. Sevetson, et al. (1995). "Identification of NAB1, a repressor of NGFI-A- and Krox20-mediated transcription." Proc Natl Acad Sci U S A **92**(15): 6873-6877.

Schippert, R., E. Burkhardt, et al. (2007). "Relative axial myopia in Egr-1 (ZENK) knockout mice." Invest Ophthalmol Vis Sci **48**(1): 11-17.

Schwachtgen, J. L., P. Houston, et al. (1998). "Fluid shear stress activation of egr-1 transcription in cultured human endothelial and epithelial cells is mediated via the extracellular signal-related kinase 1/2 mitogen-activated protein kinase pathway." J Clin Invest **101**(11): 2540-2549.

Shah, K., A. Jacobs, et al. (2004). "Molecular imaging of gene therapy for cancer." Gene Ther **11**(15): 1175-1187.

Shen, N., T. Gong, et al. (2011). "Cigarette smoke-induced pulmonary inflammatory responses are mediated by EGR-1/GGPPS/MAPK signaling." Am J Pathol **178**(1): 110-118.

Shimoyamada, H., T. Yazawa, et al. (2010). "Early growth response-1 induces and enhances vascular endothelial growth factor-A expression in lung cancer cells." Am J Pathol **177**(1): 70-83.

Silverman, E. S., J. Du, et al. (1998). "cAMP-response-element-binding-protein-binding protein (CBP) and p300 are transcriptional co-activators of early growth response factor-1 (Egr-1)." Biochem J **336 (Pt 1)**: 183-189.

Simmons, D. L., D. B. Levy, et al. (1989). "Identification of a phorbol ester-repressible v-src-inducible gene." Proc Natl Acad Sci U S A **86**(4): 1178-1182.

Stanger-Hall, K. F., J. E. Lloyd, et al. (2007). "Phylogeny of North American fireflies (Coleoptera: Lampyridae): implications for the evolution of light signals." Mol Phylogenet Evol **45**(1): 33-49.

Suehiro, J., T. Hamakubo, et al. (2010). "Vascular endothelial growth factor activation of endothelial cells is mediated by early growth response-3." Blood **115**(12): 2520-2532.

Sukhatme, V. P., X. M. Cao, et al. (1988). "A zinc finger-encoding gene coregulated with c-fos during growth and differentiation, and after cellular depolarization." Cell **53**(1): 37-43.

Svaren, J., B. R. Sevetson, et al. (1996). "NAB2, a corepressor of NGFI-A (Egr-1) and Krox20, is induced by proliferative and differentiative stimuli." Mol Cell Biol **16**(7): 3545-3553.

Swirnoff, A. H., E. D. Apel, et al. (1998). "Nab1, a corepressor of NGFI-A (Egr-1), contains an active transcriptional repression domain." Mol Cell Biol **18**(1): 512-524.

Thiel, G. and G. Cibelli (2002). "Regulation of life and death by the zinc finger transcription factor Egr-1." J Cell Physiol **193**(3): 287-292.

Thompson, J. F., L. S. Hayes, et al. (1991). "Modulation of firefly luciferase stability and impact on studies of gene regulation." Gene **103**(2): 171-177.

Topilko, P., S. Schneider-Maunoury, et al. (1998). "Multiple pituitary and ovarian defects in Krox-24 (NGFI-A, Egr-1)-targeted mice." Mol Endocrinol **12**(1): 107-122.

Tremblay, J. J. and J. Drouin (1999). "Egr-1 is a downstream effector of GnRH and synergizes by direct interaction with Ptx1 and SF-1 to enhance luteinizing hormone beta gene transcription." Mol Cell Biol **19**(4): 2567-2576.

Tsai-Morris, C. H., X. M. Cao, et al. (1988). "5' flanking sequence and genomic structure of Egr-1, a murine mitogen inducible zinc finger encoding gene." Nucleic Acids Res **16**(18): 8835-8846.

Viviani, V. R., T. L. Oehlmeyer, et al. (2005). "A new firefly luciferase with bimodal spectrum: identification of structural determinants of spectral pH-sensitivity in firefly luciferases." Photochem Photobiol **81**(4): 843-848.

Vogel, S. (2003). Characterization of signal transduction pathways in proliferating vascular smooth muscle cells and their correlation with the process of arteriogenesis. Biology. Frankfurt am Main, Johann Wolfgang Goethe University. **Dr**.

Waidmann, M. S., F. S. Bleichrodt, et al. (2011). "Bacterial luciferase reporters: The Swiss army knife of molecular biology." Bioeng Bugs **2**(1): 8-16.

Waters, C. M., D. C. Hancock, et al. (1990). "Identification and characterisation of the egr-1 gene product as an inducible, short-lived, nuclear phosphoprotein." Oncogene **5**(5): 669-674.

Wilsbacher, L. D., S. Yamazaki, et al. (2002). "Photic and circadian expression of luciferase in mPeriod1-luc transgenic mice invivo." Proc Natl Acad Sci U S A **99**(1): 489-494.

Wilson, K., J. Yu, et al. (2008). "In vitro and in vivo bioluminescence reporter gene imaging of human embryonic stem cells." J Vis Exp(14).

Wu, M., D. S. Melichian, et al. (2009). "Essential roles for early growth response transcription factor Egr-1 in tissue fibrosis and wound healing." Am J Pathol **175**(3): 1041-1055.

Yan, S. F., J. Lu, et al. (1999). "Hypoxia-associated induction of early growth response-1 gene expression." J Biol Chem **274**(21): 15030-15040.

Yang, S. Z. and S. A. Abdulkadir (2003). "Early growth response gene 1 modulates androgen receptor signaling in prostate carcinoma cells." J Biol Chem **278**(41): 39906-39911.

Zhang, H. (2004). "Id protein-firefly luciferase N-fragment & firefly luciferase C-fragment-MyoD protein."

Zhang, N., Z. Fang, et al. (2004). "Tracking angiogenesis induced by skin wounding and contact hypersensitivity using a Vegfr2-luciferase transgenic mouse." Blood **103**(2): 617-626.

Zheng, L., J. Pu, et al. (2010). "Abnormal expression of early growth response 1 in gastric cancer: association with tumor invasion, metastasis and heparanase transcription." Pathol Int **60**(4): 268-277.

8 Acknowledgements

I would like to thank PD Dr. Elisabeth Deindl and Dr. Manfred Ogris and their respective research group for data and assistance in performing the experiments discussed in this work. A special thank you goes to Judith Pagel for carrying out the immohistochemical analyses and quantitative Egr-1 levels in liver regeneration experiments mentioned. I am grateful to Christine Csapo, Mei-Ping Wu, Nanette Rinke and Alke Schropp for technical assistance. Dr Therese Manusson is gratefully acknowledged for help in isolating SMCs and Prof. Ernst Wagner for allowing the use of the animal facility at the Chair of Pharmaceutical Biotechnology. I also want to thank Triona Cummins for proofreading.

This study was in part funded by the Nanosystems Initiative Munich (NIM), the DFG research priority programme SPP1230 and the "Förderprogramm für Forschung und Lehre (FöFoLe)" of the medical faculty at the Ludwig-Maximilians-University Munich.

I also especially want to thank my parents, which supported me during my entire education and were always there for me when needed.